

Perchlorate and Radioiodide Kinetics Across Life Stages in the Human: Using PBPK Models to Predict Dosimetry and Thyroid Inhibition and Sensitive Subpopulations Based on Developmental Stage

Rebecca A. Clewell

CIIT Centers for Health Research, Research Triangle Park, North Carolina (Subcontracted to Alion Science and Technology, Inc., Dayton, Ohio, USA)

Elaine A. Merrill

Geo-Centers, Inc., Wright-Patterson AFB, Ohio, USA

Jeffery M. Gearhart and Peter J. Robinson

Alion Science and Technology, Inc., Dayton, Ohio, USA

Teresa R. Sterner

Operational Technologies Corp., Dayton, Ohio, USA

David R. Mattie

AFRL/HEPB, Wright-Patterson AFB, Ohio, USA

Harvey J. Clewell, III

CIIT Centers for Health Research, Research Triangle Park, North Carolina Subcontracted to Alion Science and Technology, Inc., Dayton, Ohio, USA

Perchlorate (ClO_4^-) is a drinking-water contaminant, known to disrupt thyroid hormone homeostasis in rats. This effect has only been seen in humans at high doses, yet the potential for long term effects from developmental endocrine disruption emphasizes the need for improved understanding of perchlorate's effect during the perinatal period. Physiologically based pharmacokinetic/dynamic (PBPK/PD) models for ClO_4^- and its effect on thyroid iodide uptake were constructed for human gestation and lactation data. Chemical specific parameters were estimated from life-stage and species-specific relationships established in previously published models for various life-stages in the rat and nonpregnant adult human. With the appropriate physiological descriptions,

these kinetic models successfully simulate radioiodide data culled from the literature for gestation and lactation, as well as ClO_4^- data from populations exposed to contaminated drinking water. These models provide a framework for extrapolating from chemical exposure in laboratory animals to human response, and support a more quantitative understanding of life-stage-specific susceptibility to ClO_4^- . The pregnant and lactating woman, fetus, and nursing infant were predicted to have higher blood ClO_4^- concentrations and greater thyroid iodide uptake inhibition at a given drinking-water concentration than either the nonpregnant adult or the older child. The fetus is predicted to receive the greatest dose (per kilogram body weight) due to several factors, including placental sodium-iodide symporter (NIS) activity and reduced maternal urinary clearance of ClO_4^- . The predicted extent of iodide inhibition in the most sensitive population (fetus) is not significant (~1%) at the U.S. Environmental Protection Agency reference dose (0.0007 mg/kg-d).

Received 4 January 2004; accepted 14 March 2006.

The authors thank Annie Jarabek, Tammy Covington, and Dr. Jeff Fisher for their advice and support of the modeling effort, and Lt. Col. Dan Rogers, Dr. Kyung Yu, Dr. Darol Dodd, and the U.S. Air Force for their support of this project. We are also indebted to Dr. John Gibbs for providing the Chilean data and Latha Narayanan for perchlorate analysis.

Address correspondence to Rebecca A. Clewell, CIIT Centers for Health Research, Six Davis Drive, Research Triangle Park, NC 27709-2137, USA. E-mail: rclewell@ciit.org

Perchlorate (ClO_4^-) is a stable anion formed from the dissociation of the oxidizing agent and rocket fuel component, ammonium perchlorate. In addition to rocket fuel, perchlorate salts are used in fireworks, ammunition, and airbags, and are a prominent

constituent of Chilean soil, from which some commercial fertilizers have originated (Collette et al., 2003; Motzer, 2001; U.S. EPA, 2003). ClO₄⁻ may be formed naturally as a product of atmospheric oxidation (Dasgupta et al., 2005). Historically, its use in rocket fuel was associated with contamination of ground and drinking-water sources throughout the western United States, though recent discovery of contamination from indeterminate sources has lent credence to the suggestion that ClO₄⁻ may be naturally occurring in more locations than had been previously assumed (Dasgupta et al., 2005). Recent findings of ClO₄⁻-contaminated produce, such as lettuce, soybeans, and tomatoes, and its presence in dairy milk suggest that sources other than drinking water may play a role in human ClO₄⁻ exposure (Jackson et al., 2005; Kirk et al., 2005; U.S. FDA, 2004).

The primary concern with regard to ClO₄⁻ exposure is the potential for endocrine disruption. ClO₄⁻ is a known inhibitor of sodium-iodide symporter (NIS), a protein in the thyroid follicle that actively transports iodide into the thyrocyte for hormone synthesis. In January 2005, the National Research Council of the National Academies released a report summarizing their characterization of the human health risk from ingestion of ClO₄⁻ in drinking water (NRC, 2005). The proposed reference dose of 0.0007 mg/kg-d, which was subsequently adopted by the U.S. Environmental Protection Agency (U.S. EPA, 2005), was based on the no-observed-effect level (NOEL) from thyroid iodide uptake inhibition studies in adult men and women (Greer et al., 2002) and a default uncertainty factor of 10 to account for intraspecies variability, particularly perinatal susceptibility. In this article, physiologically based pharmacokinetic (PBPK) models for perchlorate and iodide are described for the perinatal period in the human. Using these models, one can begin to evaluate the differences in ClO₄⁻ kinetics across life stages in order to predict the extent of perinatal susceptibility more quantitatively.

Heightened concern about thyroid inhibition in the perinatal period arises from both the dependency of development on thyroid hormones (Howdeshell, 2002; Porterfield, 1994; Thuett et al., 2002a, 2002b) and the presence of NIS in the placenta and mammary gland (Mitchell et al., 2001; Spitzweg et al., 1998; Tazebay et al., 2000). The existence of NIS in these tissues suggests that the maintenance of iodide levels is important to perinatal development, and indeed, iodide deficiency during gestation and infancy is associated with a variety of developmental defects, including congenital abnormalities, lowered IQ, and mental retardation (Delange, 2000; Dobbing, 1974; Haddow et al., 1999; Hetzel & Dunn, 1989; Klein et al., 1972; Porterfield, 1994). Because ClO₄⁻ binds NIS, there is also concern about the disruption of the developing child's iodine supply from the milk and placenta (Thuett et al., 2002b). Discovery of ClO₄⁻ in human breast milk led to further speculation about neonatal exposure (Ginsberg & Rice, 2005; Kirk et al., 2005; Tellez et al., 2005).

In the human, the effect of ClO₄⁻ exposure on thyroid hormone homeostasis is not well defined. Although radiolabeled studies suggest that the inhibition of thyroid iodide uptake is similar between the human and rat (Merrill et al., 2005a), the

effect on hormone production is quite different between the species. In human studies where adults were exposed daily to ClO₄⁻ in drinking water for 2 wk, the high-dose group (0.5 mg/kg-d) did not show significant changes in serum T₃, T₄, or thyroid-stimulating hormone (TSH) (Greer et al., 2002), but significant changes in TSH and free T₄ (but not T₃ or total T₄) were found at higher doses ClO₄⁻ after 4 wk (Brabant et al., 1992). A recent study in 13 human volunteers showed no significant changes in T₃, free T₄ or thyroglobulin concentrations after six months of exposure to 3 or 5 mg ClO₄⁻ daily (Braverman et al., 2006). In contrast, rodents appear to be more susceptible to perchlorate disruption of thyroid homeostasis. The rat shows significant hormone changes (increased TSH and free T₄) and initiation of upregulation within 24 h of ClO₄⁻ exposure at doses as low as 0.1 mg/kg-d (Yu et al., 2002). Likewise, perchlorate has been shown to affect thyroid hormone levels and thyroid histology in immature deer mice exposed in utero or via lactational transfer (Thuett et al., 2002a). The level or duration of ClO₄⁻ exposure required to induce upregulation in the human, let alone overwhelm that mechanism, is not known.

The use of physiologically based models enables us to study the impact of kinetic differences (placental and milk transfer) and the changing physiology (nonuniform tissue growth and changing clearance) on perchlorate-induced inhibition of thyroid iodide uptake. By accounting for known differences in biology between species and across life stages, it is possible to develop a quantitative estimate of risk, while minimizing uncertainty. A suite of PBPK models were previously published describing perchlorate, iodide, and inhibition kinetics in the adult male, pregnant, lactating, fetal, and neonatal rat, as well as in the adult human (Clewell et al., 2003a, 2003b; Merrill et al., 2003, 2005a). Since these models are based on measured physiological parameters, a comparison of the kinetic parameters required to reproduce various exposure data yields important information on both species and life-stage differences in chemical parameters. This article describes the manner in which the previous rat and human models were used to develop predictive models for the human gestation and postnatal period and how the resulting models were tested against available data in the perinatal human. The potential use of these models in estimating human risk is also addressed.

METHOD

Model Structure

Model Compartments

The basic structures of these human models are identical to those developed for perchlorate and iodide in the lactating and pregnant rat (Figure 1) (Clewell et al., 2003a, 2003b). A brief description follows and details of maternal compartment descriptions, including corresponding rate equations, are provided in the previous publications. Since only the thyroid is able to incorporate I⁻ into hormones, the kinetic behavior of total radioiodine was assumed to behave as free iodide in all compartments other than the thyroid. Therefore, both ClO₄⁻

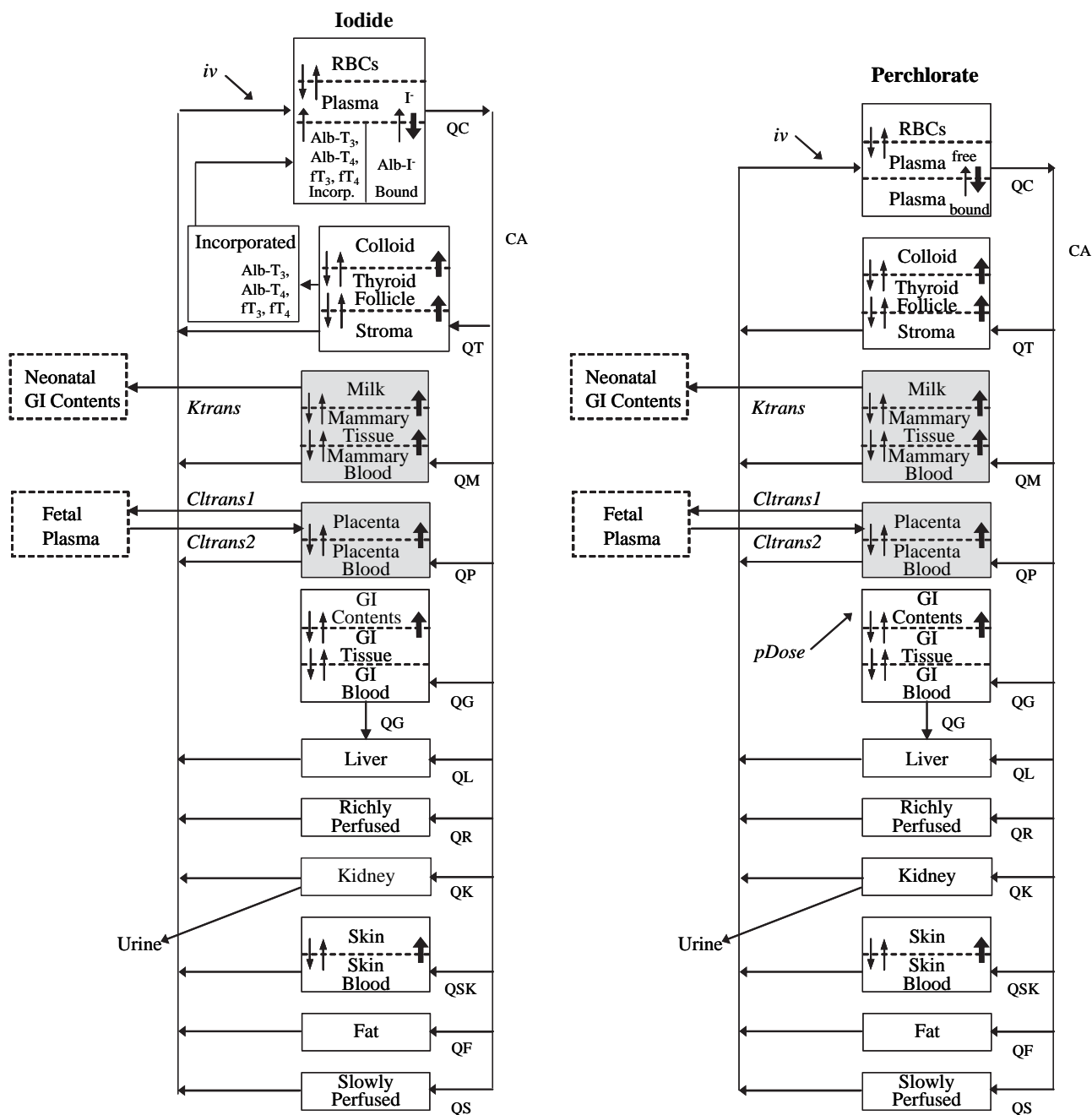


FIG. 1. PBPK models for radioiodide (left) and perchlorate (right) in the pregnant or lactating woman. The fetal and neonatal models are identical, minus the shaded compartments. The fetal model does not include incorporation of iodide into thyroid hormones as is described in the Methods section. Bold arrows indicate active transport, double arrows represent passive diffusion, and thin single arrows designate first-order rates.

and I^- could be described with the same model. The only difference in the models is the inclusion of a simple description of hormone production and secretion from the thyroid into the blood in the iodide model ($ClSecr_i$, $ClProd_i$ in Figure 1). This description was not needed in the ClO_4^- model, as perchlorate is not incorporated into hormones.

Compartments for the thyroid, skin, stomach, mammary gland, placenta, and milk were included in the maternal models

based on the presence of NIS and their ability to affect I^- kinetics (Brown-Grant, 1961; Brown-Grant & Pethes, 1959; Halmi & Stuelke, 1959; Kotani et al., 1998; Spitzweg et al., 1998; Wolff, 1998). Three compartments were used to describe the thyroid stroma, follicle and colloid. In the iodide model only, an additional subcompartment was included in the thyroid to account for incorporation of I^- into hormones. The intestine (gastrointestinal tract, GI) was also represented by three

compartments: the capillary bed, tissue, and GI contents. The skin, placenta, and mammary gland were each split into two compartments, representing the capillary blood and tissue. In lactation, the mammary gland has an additional milk compartment. NIS-mediated uptake was described with Michaelis–Menten kinetics (bold arrows in Figure 1). Permeability area cross products and partition coefficients describe passive diffusion of the anions between the blood, tissues, and inner compartments (small arrows). The kidneys, liver, fat, and richly and slowly perfused tissues were described using flow-limited transfer.

For both models, the blood has three separate compartments: free anion in the red blood cells and plasma, and protein-bound anion in the plasma. In the iodide model, the “plasma bound iodine” compartment represents all forms of iodine other than free inorganic iodide—including albumin-bound I⁻, free and protein-bound T₃ and T₄, and iodinated hormone precursors. Hormone iodine is secreted into the “plasma bound iodide” compartment from the “thyroid incorporated iodine” compartment and is then lost to the free plasma iodide compartment using a first-order rate to approximate peripheral deiodination.

The structures of the fetal and neonatal models are the same as for the perinatal woman, with the exception of the mammary gland and placenta compartments. Fetal exposure is described as a first-order transfer from the placenta to the serum of the fetus. Clearance in the fetus is described as first-order loss from the fetal serum to the placenta. Due to the lack of data from either rat or human studies, binding of iodine was not described in the fetal thyroid and plasma. Neonatal dose is based on predicted milk concentrations and measured ingestion rates in human infants. Hormone production and secretion, serum binding, and urinary excretion in the neonate are modeled in the same manner as the maternal model.

Perchlorate-Induced Inhibition of Iodide Uptake via NIS

Inhibition of iodide uptake was included in the maternal, neonatal, and fetal thyroid follicle and colloid, GI contents, and skin, as well as the maternal placenta, mammary gland, and milk, based on various literature sources showing inhibition in these tissues in laboratory animals and humans (Clewell et al., 2003a, 2003b; Halmi & Stuelke, 1959; Merrill et al., 2003). Competitive inhibition of I⁻ by ClO₄⁻ was modeled by adjusting the K_{mi} by one plus the serum [ClO₄⁻]: K_{mp} ratio [Eq. (1)] as described in the previous models (Clewell et al., 2003a, 2003b).

$$RupTF_i = \frac{V \max TF_i * CTS_i}{KmTF_i * \left(1 + \frac{CTS_p}{KmTF_p}\right) + CTS_i} \quad [1]$$

$RupTF_i$ represents the rate of active iodide uptake into the thyroid follicle. This rate is modified by the affinity of transport mechanism in the follicle for ClO₄⁻ ($KmTF_p$) and the

concentration of ClO₄⁻ in the stroma (CTS_p). Inhibition of iodide uptake in other tissues with NIS is described in the same manner as the thyroid follicle inhibition.

Simulating Dose Administration

In order to estimate exposures from drinking water, the women were assumed to drink at a constant rate for 24 h/d. This method provides an estimate of average tissue ClO₄⁻ concentrations at steady state. A pulse function in ACSL (Advanced Continuous Simulation Language, AEGIS Technologies Group, Inc., Huntsville, AL) was used to introduce drinking water to the mother’s stomach contents for both drinking-water and acute oral dosing regimens. Intravenous (iv) dosing was introduced into the venous blood compartment of the model. The fetus was continuously exposed to maternal perchlorate and iodine via the placenta. Neonatal dose was modeled as entering the stomach contents at the suckling rate (Gentry et al., 2002). Direct doses were also introduced into the venous blood compartment of the neonate when iv dosing was used in the associated literature study.

Model Parameters

Whenever possible, model parameters were taken from literature data and allometric scaling was employed to account for the change in parameters resulting from variations in body weight (BW). Values for blood flows (Q), permeability area cross products (PA), clearance rates (Cl), and maximum velocities (V_{max}) were scaled by $BW^{0.75}$. The model was programmed in ACSL. Examples of the model equations that have not been previously published are given in the Appendix.

Physiological Parameters

In addition to total body weight changes in the woman and offspring, cardiac output, fractional body fat, placenta, mammary tissue, and milk production also change with respect to time. Fetal/neonatal body weight and fractional body fat are also highly dynamic. Growth equations based on Gentry et al. (2002) and various published data sets (described later) were used to account for these changes. Blood flows and remaining tissue volumes were adjusted with respect to the changing parameters.

Maternal tissues and blood flows. Allometric scaling alone does not sufficiently describe the physiological changes taking place during the perinatal period. During gestation, the placenta, uterus, mammary gland, and fetal volume are growing at an accelerated rate. Likewise, the mammary gland, maternal and neonatal fat content, and neonatal body weight show the most dramatic changes during lactation. Since growth of other tissues is negligible in comparison to those just described, the total change in the maternal body weight is simply described as the change added to the initial (pregnancy/at birth) body weight (BW_{init}). All other maternal organs are assumed to

remain constant and are scaled from the nonpregnant adult value (Merrill et al., 2005a) by $BW_{\text{init}}^{0.75}$.

The equations for the growth of the maternal mammary gland, fat, uterus, and placenta in pregnancy and the fat and mammary gland in lactation are available in Gentry et al. (2002). The uterus is not a defined compartment in this gestation model due to the lack of chemical distribution data in either species. However, it was necessary to describe the physical growth of the uterus in order to estimate the total growth of the pregnant woman. The uterus was then lumped with the richly perfused tissue for kinetic simulations.

Temporal changes in maternal cardiac output during the perinatal period are simulated by adding the change in blood flow to the mammary, fat, placenta, and uterus to the initial cardiac output (Gentry et al., 2002). The changes in fractional blood flow (%BW) to these tissues are considered to be proportional to the changes in tissue volume. The change in blood flow to the placenta is also linearly related to the change in the volume.

Fetal tissues. Fetal growth was described with the Gompertz equation reported in Gentry et al. (2002) and Shipp et al. (2000). Fetal thyroid and relative stroma, follicle, and colloid volumes were based on the data of Bocian-Sobkowska et al. (1992, 1997) as described in the Appendix. All other fetal tissues were scaled allometrically from the adult fractional volumes (Merrill et al., 2005a).

Neonate/child tissues. Since fractional blood (per kg BW), plasma, and red blood cell (L blood) volumes were measured in children from birth to 18 yr and no significant difference was found with age (Brines et al., 1941), neonatal blood volumes were scaled from the adult values. The equations for the increase in total body weight and richly perfused tissues from birth through adulthood were given in Clewell et al. (2004). Fat, skin, kidneys, liver, and stomach volume from birth to 18 yr were described according to the equations of Haddad et al. (2001). Total thyroid volumes in children from birth to 17 yr were reported by Ogiu et al. (1997). Fractional stroma, follicle, and colloid volumes at birth were given in Bocian-Sobkowska et al. (1997) and in children from 1 to 20 yr in Brown et al. (1986). Model descriptions of the total and fractional thyroid volumes are given in the Appendix.

Chemical-Specific Parameters

Estimated parameters. Much of the data required to determine chemical specific parameter values, such as clearance values and partition coefficients, were not available in the perinatal human. Most of the parameters were therefore estimated from previous rat life-stage and adult human ClO_4^- models using the parallelogram approach described in Clewell et al. (2001). For a particular parameter, the ratio of the value in the perinatal model to its value in the adult male rat yielded a “life-stage-specific adjustment factor.” Likewise, the ratio of the values used in the adult male rat and adult human generated a “species-specific adjustment factor.” Applying these two

adjustment factors to the value in the adult male rat produced an estimated parameter value for the perinatal human, as shown in Eq. (2).

$$\begin{aligned} V \max cTF_{i(\text{male rat})} &\times \text{Life-stage adjustment} \\ &\times \text{Species adjustment} \\ &= V \max cTF_{i(\text{pregnant human})} \end{aligned} \quad [2]$$

For example, thyroidal uptake of I^- showed both life-stage- and species-specific differences in the previous models. The value for follicular I^- uptake ($V \max cTF_i$) was 5.4×10^4 ng/L-h in the male rat and 1.5×10^5 ng/L-h in the human, resulting in a “species-specific adjustment factor” of 2.8. The same parameter was only 4.4×10^4 ng/L-h in the pregnant rat, giving a “life-stage-specific adjustment factor” of 0.82. By applying these two factors to the male rat value, an estimate was generated for the corresponding parameter in a pregnant human (1.2×10^5 ng/L-h), as shown in Eq. (3).

$$\begin{aligned} V \max cTF_{i(\text{pregnant human})} &= (5.4 \times 10^4) \times (0.82) \times (2.8) \\ &= 1.2 \times 10^5 \text{ ng/L-h} \end{aligned} \quad [3]$$

This same process was applied to obtain all chemical-specific parameters for both anions (Tables 1 and 2), unless otherwise indicated by the literature. Exceptions are described next.

In the neonatal model, some of the parameters could not be directly estimated from the rat, due to the fact that the newborn rat is physically less mature than the human (the neonatal rat is roughly equivalent to the late gestation human fetus). Furthermore, as the period of lactation in the human covers the first year of life, it is expected that many parameters are changing over time. Two such parameters are those describing urinary clearance and serum binding. In the rat, both of these parameters were lower in the neonate than in the adult based on the fit of the model to the data. In the human, it was necessary to use a different approach. Age-related changes in serum binding were assumed to be proportional to the change in binding protein concentration. Since both albumin (Kurz et al., 1977; Stewart & Hampton, 1987) and thyroid binding globulin (TBG) (Fisher & Nelson, 2001) concentrations do not change significantly between birth and adulthood, the parameters for plasma binding of both anions were set to the adult value and scaled allometrically to account for growth. Likewise, kidney function was assumed to be proportional to blood flow. Thus, the parameter describing clearance (ClUc) was scaled by $BW^{0.75}$ from the adult value to account for growth-related changes.

The species difference in placental and mammary gland NIS could not be estimated from the adult human model (Merrill et al., 2005a), since the placenta is not present and NIS is inactive in the mammary gland of the normal adult.

TABLE 1
Perchlorate Chemical-Specific Parameters

Parameters	Gestation		Lactation	
	Woman	Fetus	Woman	Neonate
Gastric tissue/gastric blood <i>PG</i>	1.29 ^a	1.79 ^a	4.6 ^a	8.25 ^a
Gastric juice/gastric tissue <i>PGJ</i>	1.76 ^a	21.3 ^a	3.1 ^a	7.63 ^a
Skin tissue/skin blood <i>PSk</i>	1.32 ^a	1.32 ^a	1.32 ^a	1.32 ^a
Mammary tissue/ mammary blood <i>PM</i>	0.66 ^b	—	0.66 ^b	—
Mammary/milk <i>PMk</i>	—	—	2.39 ^b	—
Placenta/placental blood	0.56 ^b	—	—	—
Maximum capacity (ng/h/kg)				
Thyroid follicle <i>VmaxcTF</i>	6.0 × 10 ^{3a}	0 – 2 × 10 ^{5e}	9.0 × 10 ^{3a}	0.6–2.4 × 10 ^{5e} /6 × 10 ^{3c}
Thyroid colloid <i>VmaxcTL</i>	1.7 × 10 ^{4a}	1.7 × 10 ^{4a}	8.4 × 10 ^{3a}	1.7 × 10 ^{4a}
Skin <i>VmaxcS</i>	1.2 × 10 ^{6a}	8.0 × 10 ^{5a}	1.6 × 10 ^{6a}	1.6 × 10 ^{6a}
GI <i>VmaxcG</i>	3.2 × 10 ^{7a}	4.0 × 10 ^{6a}	5.0 × 10 ^{6a}	5.0 × 10 ^{6a}
Mammary <i>VmaxcM</i>	2.2 × 10 ^{4b}	—	2.0 × 10 ^{4b}	—
Milk <i>VmaxcMk</i>	—	—	2.0 × 10 ^{4b}	—
Placenta <i>VmaxcP</i>	6.0 × 10 ^{4b}	—	—	—
Affinity constants (ng/L)				
Mammary <i>KmM</i>	2.0 × 10 ^{5c}	—	2.0 × 10 ^{5c}	—
Milk <i>KmMk</i>	—	—	1.0 × 10 ^{6b}	—
Placenta <i>KmP</i>	2.0 × 10 ^{5c}	—	—	—
Permeability area cross products, (L/h-kg)				
Gastric blood to gastric tissue <i>PAGc</i>	0.6 ^a	0.6	0.6	0.6 ^a
Gastric tissue to gastric juice <i>PAGJc</i>	1.0 ^a	1.0	1.0	1.0 ^a
Thyroid blood to thyroid tissue <i>PATFc</i>	1.0 × 10 ^{-4a}	1.0 × 10 ^{-2f}	6.7 × 10 ⁻⁵	6.7 × 10 ^{-5a}
Thyroid follicle to thyroid lumen <i>PATLc</i>	0.01 ^a	0.01 ^a	0.01	0.01 ^a
Skin blood to skin tissue <i>PASkc</i>	1.25 ^a	1.25 ^a	0.63	1.25 ^a
Mammary blood to mammary tissue <i>PAMc</i>	0.04 ^a	—	0.01	—
Mammary tissue/milk <i>PAMkc</i>	—	—	0.1	—
Placenta blood to placenta <i>PAPCc</i>	0.1 ^b	—	—	—
Clearance values, (L/h-kg)				
Urinary excretion <i>CLUc</i>	0.05 ^d	—	0.05 ^d	0.13 ^c
Placenta to fetal blood <i>Cltrans1c</i>	—	0.12 ^f	—	—
Fetal blood to placenta <i>Cltrans2c</i>	—	0.12 ^b	—	—
Binding constants				
<i>VmaxcB</i>	5.9 × 10 ^{2a}	5.0 × 10 ^{2c}	1.32 × 10 ^{3a}	5.0 × 10 ^{2c}

Note. Partition coefficients for perfusion limited compartments (i.e., fat, liver, kidney, rapidly and slowly perfused tissues) were the same across species and life stages.

^aCalculated using parallelogram approach.

^bSet to rat value (in absence of equivalent human parameter).

^cSet to adult human value.

^dAdjusted to fit data set.

^eCalculated from human perinatal iodide parameter and ClO₄⁻:I⁻ ratio in adult.

^fSet to human perinatal iodide value (in absence of equivalent perchlorate data).

Thus, parameters describing NIS-mediated uptake of I⁻ and ClO₄⁻ into the placenta (*VmaxcP*), mammary gland (*VmaxcM*) and milk (*VmaxcMk*) were scaled allometrically from those determined for the pregnant and lactating rat (Clewell et al., 2003a, 2003b). The affinity constants for NIS were assumed

to be similar across species and life stages in all of the models based on measurements in different tissues and species (Gluzman & Niepomnische, 1983; Wolff, 1998). Therefore, the *K_m* values reported by Merrill et al. (2005a) for the thyroid (1.5 × 10⁵ ng/kg-h) and extrathyroidal

TABLE 2
Iodide Chemical-Specific Parameters

Parameters	Gestation		Lactation	
	Woman	Fetus	Woman	Neonate
Gastric tissue/gastric blood <i>PG</i>	1.0 ^a	1.0 ^a	0.5 ^a	0.6 ^a
Gastric juice/gastric tissue <i>PGJ</i>	2.0 ^a	2.0 ^a	1.0 ^a	1.0 ^a
Skin tissue/skin blood <i>PSk</i>	1.0 ^a	1.0 ^a	1.0 ^a	1.0 ^a
Mammary tissue/mammary blood <i>PM</i>	0.66 ^b	—	0.8 ^b	—
Mammary/milk <i>PMk</i>	—	—	1.0 ^b	—
Placenta/placental blood	0.40 ^b	—	—	—
Maximum capacity (ng/h/kg)				
Thyroid follicle <i>VmaxcTF</i>	1.22 × 10 ^{5a}	0 – 5.0 × 10 ^{6d}	1.4 × 10 ^{5a}	1.5–6 × 10 ^{6d} /1.5 × 10 ^{5c}
Thyroid colloid <i>VmaxcTL</i>	1.0 × 10 ^{8a}	1.0 × 10 ^{8a}	1.0 × 10 ^{8a}	1.0 × 10 ^{8a}
Skin <i>VmaxcS</i>	7.2 × 10 ^{4a}	8.4 × 10 ^{5a}	5.6 × 10 ^{5a}	3.5 × 10 ^{5a}
GI <i>VmaxcG</i>	4.6 × 10 ^{5a}	9.0 × 10 ^{5a}	9.0 × 10 ^{5a}	9.0 × 10 ^{5a}
Mammary <i>VmaxcM</i>	4.0 × 10 ^{4a}	—	8.0 × 10 ^{5b}	—
Milk <i>VmaxcMk</i>	—	—	5.0 × 10 ^{5b}	—
Placenta <i>VmaxcP</i>	5.5 × 10 ^{4b}	—	—	—
Affinity constants, <i>Km</i> (ng/L)				
Mammary <i>KmM</i>	4.0 × 10 ^{6b}	—	4.0 × 10 ^{6b}	—
Milk <i>KmMk</i>	—	—	1.0 × 10 ^{7b}	—
Placenta <i>KmP</i>	4.0 × 10 ^{6b}	—	—	—
Permeability area cross products (L/h·kg)				
Gastric blood to gastric tissue <i>PAGc</i>	0.16 ^a	0.12 ^a	0.16 ^a	0.01 ^a
Gastric tissue to gastric juice <i>PAGJc</i>	12.0 ^a	0.3 ^a	12.0 ^a	1.8 ^a
Thyroid blood to thyroid tissue <i>PATFc</i>	1.0 × 10 ^{-4a}	1.0 × 10 ^{-2d}	1 × 10 ^{-4a}	1.0 × 10 ^{-4a}
Thyroid follicle to thyroid lumen <i>PATLc</i>	1.5 × 10 ^{-5a}	1.0 × 10 ^{-4a}	2.0 × 10 ^{-3a}	1.25 × 10 ^{-3a}
Skin blood to skin tissue <i>PASkc</i>	0.06 ^a	0.06 ^a	0.12 ^a	0.012 ^a
Mammary blood to mammary tissue <i>PAMc</i>	0.01 ^b	—	0.02 ^b	—
Mammary tissue/milk <i>PAMkc</i>	—	—	0.02 ^b	—
Placenta blood to placenta <i>PAPCc</i>	0.005 ^b	—	—	—
Clearance values (L/h·kg)				
Urinary excretion <i>CLUc</i>	0.05 ^a	—	0.1 ^a	0.1 ^c
Placenta to fetal blood <i>CLtrans1c</i>	—	0.12 ^d	—	—
Fetal blood to placenta <i>CLtrans2c</i>	—	0.12 ^b	—	—

Note. Partition coefficients for perfusion limited compartments (i.e., fat, liver, kidney, rapidly and slowly perfused tissues) were the same across species and life stages.

^aCalculated using parallelogram approach.

^bSet to rat value (in absence of equivalent human parameter).

^cSet to adult human value.

^dAdjusted to fit data set.

tissues (2.0×10^5 ng/kg-h) were used for all life-stages. In addition to NIS, a pendrin-iodide transporter was identified in the mammary gland (Rillema and Hill, 2003), and was included in both the rat and human models. Since no human measure of this transporter's activity was available, the affinity was assumed to be the same as the rat (Clewell et al., 2003a). Diffusion parameters in the placenta and mammary gland and milk kinetics were also scaled allometrically ($BW^{0.75}$) from the rat. No data were found indicating

a need for additional species adjustment factors with these parameters.

Fitted parameters. Only the fetal thyroid parameters for follicular uptake (*VmaxcTF*) and permeability (*PATFc*) and the parameter for placental transfer (*CLtrans1*) were fitted to data in the human gestation model; all others were calculated from the previous models or separate data as described earlier. Placental transfer was adjusted to account for species differences based on literature data. In the previously described rat gestation

model, the transfer rates of the anions into the fetal blood from the placenta (*CLtrans1*) and into the placenta from the fetal blood (*CLtrans2*) were fit in order to achieve the experimental fetal:maternal serum ratio of 0.7 (Clewel et al., 2003b). In the human, *CLtrans1* was adjusted to yield a fetal:maternal serum ratio of ~3.0 at 18 h postdosing as indicated by the data of Dyer et al. (1969). The transfer rates for perchlorate were assumed to be the same as for I⁻.

Since the timing of gestation and that of fetal development are quite different in the rat and human, the ontogenesis of fetal thyroid uptake could not be adequately described by scaling the corresponding kinetic parameters from the rat model. Therefore, the values for *VmaxTF_i* and *PATF_i* were determined by fitting the model simulation to available radioiodide data at various weeks in gestation (not shown). Partition coefficients and the parameters for sequestration of iodine in the colloid were scaled from the adult. This is consistent with the method used in the rat and nonpregnant human models to account for variations in thyroid parameters.

The highly dynamic development of the thyroid, begun in utero, continues during the first week of life. Thyroid uptake data in infants suggest that during the first 3 d after birth, the newborn experiences a surge of thyroidal activity, resulting in dramatically increased values for 24-h thyroid uptake (Figure 2). To account for this phenomenon, it was necessary to fit the neonatal thyroid parameters to available data during the first few postnatal days. In keeping with the method used in the fetal model, only the value for the follicular *V_{max}* was adjusted to fit the average measured 24-h thyroid radioiodide. Although it is possible that the other parameters (colloid uptake,

hormone binding) may also be changing, the lack of data for thyroid subcompartments (follicle, colloid, incorporated iodine) and the inability of the model to describe detailed hormone (T₃, T₄) kinetics preclude the validation of these intrathyroidal parameters. Thus, for the sake of consistency between models, for model simplicity, and in an effort to limit the number of unverified model parameters, no other parameters were changed. After postnatal day (PND) 3, neonatal thyroid uptake measurements are indistinguishable from those in later childhood, adolescence or adulthood (Figure 2). Therefore, the neonatal *VmaxTF* values were scaled allometrically from the adult parameters after the third day of life. For both the fetus and newborn (PND 1–3), the thyroid ClO₄⁻ parameters were calculated by adjusting the fitted iodide parameter value by the ratio of ClO₄⁻:I⁻ for the same parameters in the adult human thyroid model (Merrill et al., 2005a).

Weaning was assumed to occur at 1 yr postpartum and was simulated by stopping milk production at that time. As noted earlier, at 1 wk postpartum, the neonate's thyroid I⁻ uptake does not change significantly. Therefore, thyroid uptake parameters were scaled allometrically from the adult (Merrill et al., 2005a). Chemical-specific parameters for skin and GI were also set to adult values, due to a lack of data indicating age-dependent NIS activity. As in the neonate, serum binding and urinary clearance parameters were scaled from the adult values. Thus, the physiological changes were assumed to account for any differences in I⁻ and ClO₄⁻ kinetics that may exist between weaning and adulthood.

RESULTS

Iodide Model Parameterization

Gestation Model

Fetal thyroid iodide uptake. The data from several literature studies were used to determine the fetal thyroid parameters, including data from Aboul-Khair et al. (1966), Chapman et al. (1948), Evans et al. (1967), and Hodges et al. (1955), in which women were given a single dose of radiolabeled iodine prior to termination of pregnancy. The data reported in these papers showed significant scatter in the measured values. Therefore, rather than fit one set of limited data, the data from all of the available studies were normalized to a common dose (100 ng ¹³¹I⁻). Parameters for *VmaxcTF_i* that provided the best fit to the data are shown in Figure 3.

The fetal *V_{max}* increases through the wk 32 of gestation before dropping in accordance with the decrease in observed radioiodide uptake (Figures 3 and 4). The fitted value of *V_{max}* during the last week of gestation (gestation week [GW] 40) is the same value used at birth in the lactation model (1.5 ng/L-h). In order to reproduce the increased clearance of the fetal thyroid due to lack of organification in early gestation, the value for *PATc_i* was increased to 0.01 instead of the adult of value of 0.0001 ng/h-kg. Thus, the overall trend in Figure 4 suggests

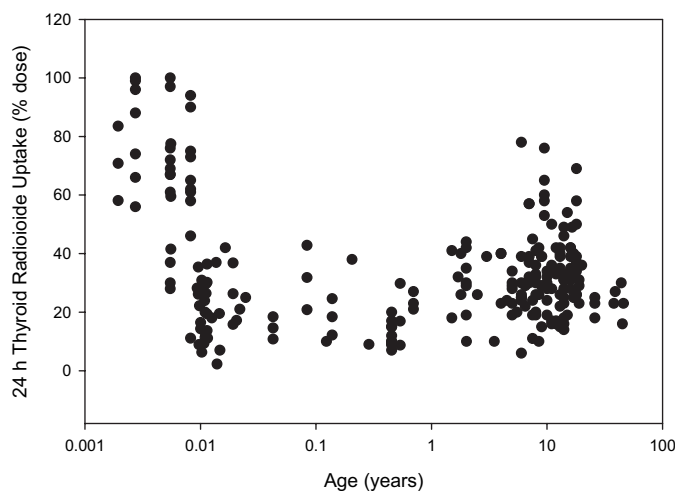


FIG. 2. Measured 24-h thyroid radioiodide uptake (% dose) in the human from birth to 48 yr. Data shown were obtained from Fisher and Oddie (1964), Kearns and Phillipsborn (1962), Martmer et al. (1956), Ogborn et al. (1960), Oliner et al. (1957), Quimby and McCune. (1947), Reilly and Bayer (1952), Van Dilla and Fulwyler (1964), Van Middlesworth et al. (1953), Fisher et al. (1962), and Wellman et al. (1970).

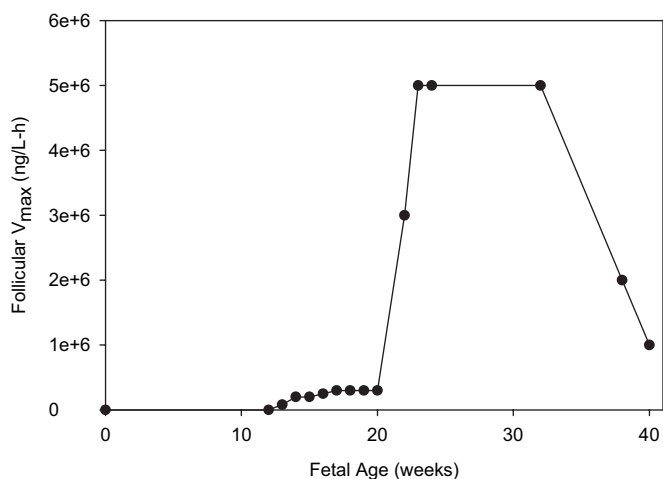


FIG. 3. Final values for fetal thyroid V_{\max} over gestation. The data points represent the values for follicular V_{\max} that were adjusted to obtain the best visual fit of the model simulated fetal thyroid iodide to the combined data for GW 13 to 38. The line represents the values estimated by linear interpolation using a TABLE function in ACSL.

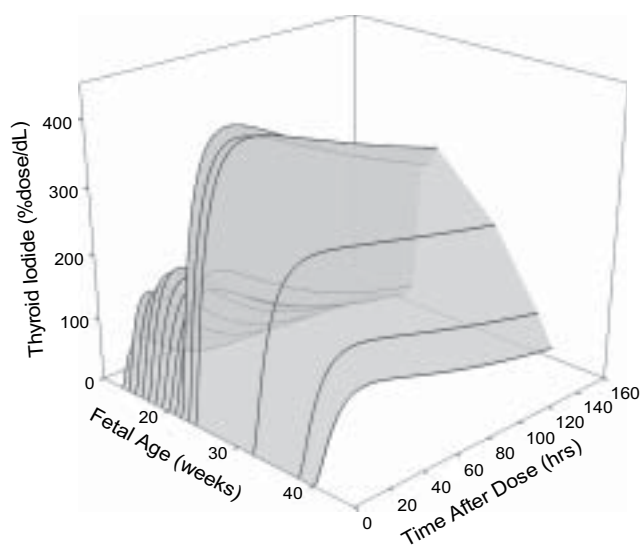


FIG. 4. Model-simulated fetal thyroid iodide concentration versus time after maternal ^{131}I dose at different weeks in gestation. The model predicts a slower release of iodide from the thyroid with increased fetal age, while the maximum thyroid concentrations peak at mid-gestation and decline during the second half of gestation.

an increased half-life for iodine in the thyroid with increasing fetal age. Though accomplished using a simplified description, the trend of the model reflects the expected physiology as the thyroid-pituitary axis matures and the fetal thyroid begins to accumulate I^- , synthesize hormones, and build up hormone stores.

Postnatal Model

Neonatal thyroid iodide uptake. Increased thyroid I^- uptake in the newborn was simulated by fitting the follicular V_{\max} to the published data in neonates given a single direct dose of radioiodide, yielding values of 1.5×10^6 , 6.0×10^6 , and 1.5×10^6 ng/hr/kg on PND 1, 2 and 3, respectively. After PND 3, $V_{\max}cTF_i$ was scaled allometrically from the adult value of 1.5×10^5 ng/h/kg. Model simulations during the first week of life are shown in Figure 5.

Iodide Model Validation

Gestation Model

Maternal tissues. Maternal tissue predictions were compared to measured $^{131}\text{I}^-$ levels in maternal thyroid, urine, placenta and blood after a single oral dose (Figure 6). The data from all available studies were mathematically converted to reflect a normalized dose (100 ng $^{131}\text{I}^-$), so the model simulation could be viewed against all data simultaneously. Since neither model-predicted nor measured iodide changed noticeably over gestation, the simulation at one representative week (GW 22) is shown versus the combined data from GW 6 to 38.

The model reproduced maternal thyroid uptake without any parameter adjustment (Figure 6A). Running the model simulation at several different time points in gestation showed no difference in predicted thyroid uptake. Likewise, the $^{131}\text{I}^-$ data showed no appreciable trend in thyroid uptake between GW 6 and 32. There was, however, a large amount of variability

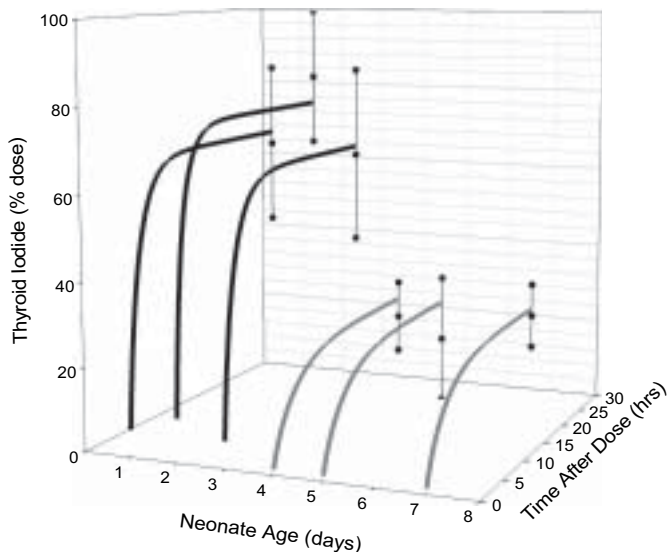


FIG. 5. Model-simulated thyroid radioiodide uptake 24 h postdosing in the newborn infant. Model simulations on PNDs 1–3 (black lines) are based on fitted values for $V_{\max}cTF_i$. Simulations of PNDs 4–7 (grey lines) are predicted from the adult parameters. Cross bars represent the mean \pm SD of the combined data (Fisher & Oddie, 1964; Kearns & Philipsborn, 1962; Martner et al., 1956; Ogborn et al., 1960; Van Middlesworth, 1954).

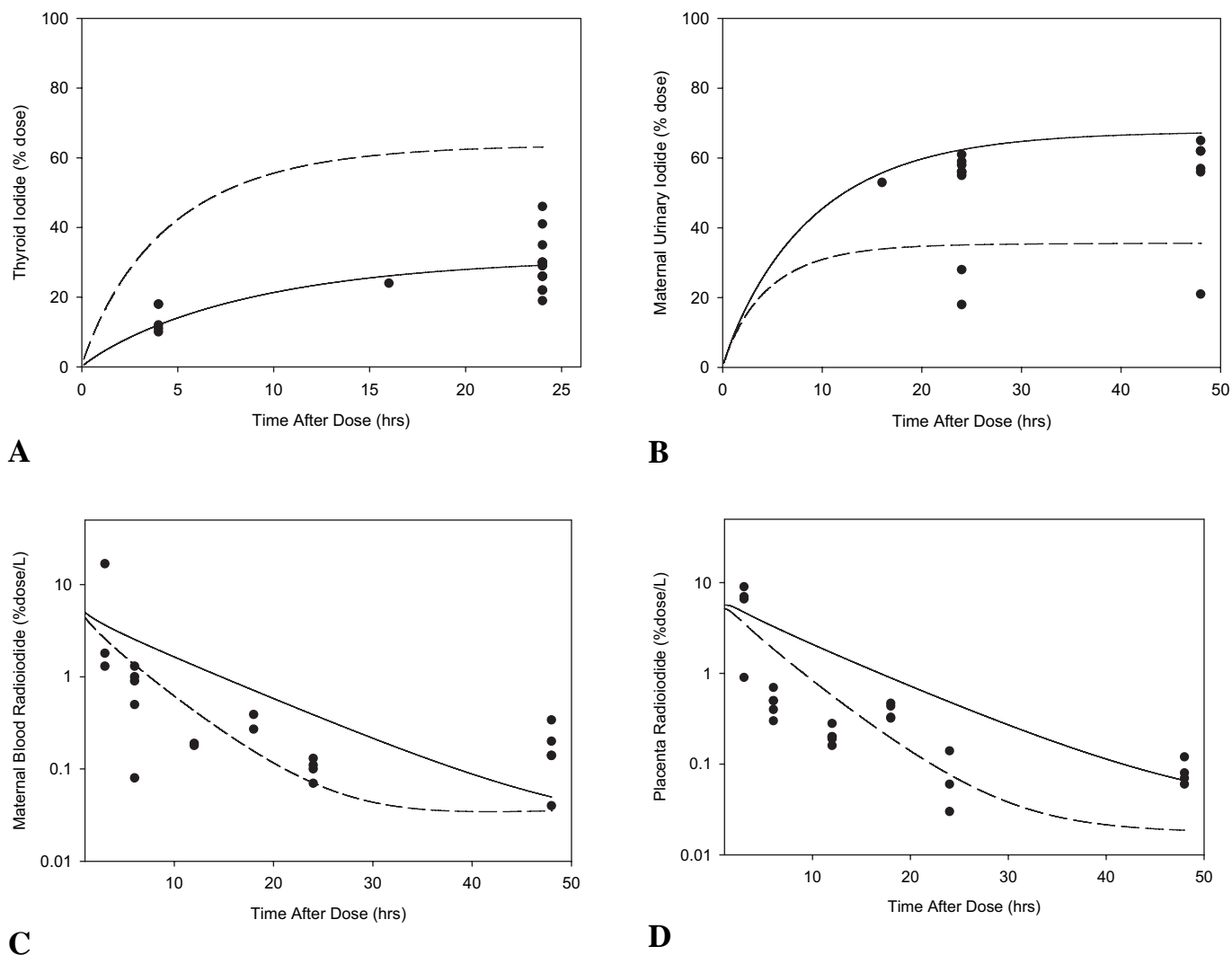


FIG. 6. Predicted radioiodide concentration in maternal (A) thyroid, (B) urine, (C) whole blood, and (D) placenta. PBPK model was run at GW 22. Data points represent individual subjects from the combined data for the thyroid (Evans et al., 1967; Hodges et al., 1955; Sternberg, 1973), urine (Chapman et al., 1948), and placenta and plasma (Aboul-Khair et al., 1966; Dyer et al., 1969), independent of the gestation week. For this and subsequent plots of maternal iodide kinetics, the solid and broken lines indicate the model simulation using the follicular $V_{max}cTF_i$ value ($V_{max}cTF_i$) calculated from the mean and maximum value, respectively, in the nonpregnant adult as reported in Merrill et al. (2005a).

between subjects; reported 24-h uptake ranged from 19 to 46% of the administered dose.

In their effort to simulate thyroid radioiodide uptake data from adult men and women, Merrill and coauthors (2005a) noted significant interindividual variability in thyroid uptake measurements that could not be explained by differences in gender, physiology (i.e., weight), or dosing regimen. Fitting baseline I^- uptake for each individual subject gave $V_{max}cTF_i$ values ranging from 33 to 800 $\mu\text{g}/\text{h}/\text{kg}$. This amounts to a 24-fold difference in the parameter that was determined to be responsible for thyroid I^- uptake in healthy, nonpregnant adults through a formal sensitivity analysis of model parameters (Merrill et al., 2005a). It follows then that the range for this parameter would be similar in magnitude in pregnant

women. As the purpose of this exercise was to test the model's utility for predictions, the parameters were not fitted to individual subjects with this model. Instead, the mean value reported by Merrill et al. (2005a) was used, and was adjusted only for the life-stage-specific differences observed in the male and pregnant rat. Nonetheless, in an effort to understand better how such variability in thyroid uptake would affect overall iodide kinetics, the model was run again using a life-stage-adjusted value for $V_{max}cTF_i$ calculated from the highest value reported by Merrill et al. (2005a). For Figure 6A and subsequent plots of maternal iodide kinetics, the solid line indicates the model simulation using the follicular V_{max} value calculated from the mean, and the broken line represents the model simulation using the follicular

V_{max} calculated from the maximum value in the nonpregnant adult.

The maternal urinary clearance value (Cl_{uc}) was set at 60% of the value in the nonpregnant human based on observed difference in the pregnant and male rat models (Clewell et al., 2003b; Merrill et al., 2003). Figure 6B shows model simulations of the maternal urine versus the data of Chapman et al. (1948) at 24 and 48 h after iv injection of $^{131}\text{I}^-$ at GW 14.5, 16, 20, and 32. Additionally, the data of Sternberg (1973) are shown at 16 h after maternal $^{131}\text{I}^-$ iv exposure on GW 14. Like the thyroid, predicted and measured urinary iodide did not change over gestation. Epidemiological studies have also shown similar urine iodine levels during the first and third trimesters (Caron et al., 1997).

Model predictions of the maternal blood and placenta iodide levels after a single dose are shown in Figures 6C and 6D. The blood iodide and, consequently the placenta iodide concentrations, are highly dependent on thyroid uptake. When the model is run using the higher value for V_{maxcTF_i} , the blood and placenta predictions fall more completely within the data. This suggests that a higher value of V_{maxcTF_i} may be appropriate for the pregnant woman. However, as it stands, the model predicts maternal kinetics reasonably well based on the previously validated rat and nonpregnant human models without post hoc manipulation of parameters.

Fetal tissues. The ability of the model to predict human fetal kinetics and the placental-fetal iodide transfer after GW 12 (onset of NIS activity) was tested against the data available for total fetal $^{131}\text{I}^-$ body burden as well as the few data available for individual tissues in the fetus. In the studies published by Aboul-Khair et al. (1966) and Dyer and Brill (1972), total radiolabeled iodide in the fetal body was reported at various weeks of gestation after maternal iv dose. Figure 7 illustrates the model-predicted body burden of the fetus compared to the individual data from these two studies. While the model curve shows the iodide time course after an acute dose to a single subject, the data represent a different individual subject for each point shown. The model appears to follow the same trend as the data, and in most cases is within the range of the measured values. Notable exceptions are GW 18 and 19. However, these particular data points are quite low and appreciably different from the other data sets. Thyroid measurements taken in the same fetuses (not shown) are quite high, suggesting that these low levels may be due to experimental artifact.

The data of Dyer et al. (1969) were not included in those used previously to fit the fetal thyroid parameters, and was therefore used to test the fetal thyroid predictions. Fetal blood, GI, and kidney were also available at GW 14, 15 and 22 after a single maternal oral $^{131}\text{I}^-$ dose. These tissue levels are predicted remarkably well, not only in the thyroid, but also in the blood, GI, and kidney (Table 3). Only the kidney and GI on GW 14 are more than twofold different from measured values.

Postnatal Model

Maternal tissues. The kinetic behavior of radioiodide in the lactating woman appears to be independent of the time in lactation during which the isotope is administered. From the compiled literature data, there is no apparent trend in thyroid uptake, cumulative urine or milk concentration over the course of lactation. The model predictions of these dose metrics also remain constant. Thus, the following model simulations of maternal radioiodine kinetics are shown at one representative month (postnatal month [PNM] 4) versus the combined data normalized to a dose of 100 ng $^{131}\text{I}^-$.

Maternal thyroid uptake, cumulative urine, and milk radioiodine are shown in Figure 8. Based on the adult male and lactating rat models (Clewell et al., 2003a; Merrill et al., 2003), the maternal parameter for follicular uptake (V_{maxcTF_i}) was quantitatively lower than the average value in the adult male. The model was also run using a V_{maxcTF_i} calculated from the maximum value reported by Merrill et al. (2005a). Without altering any of the previously calculated parameters, the model simulation bracketed the range of the reported data for radioiodide accumulation in the maternal thyroid up to 48 h postdosing using these two values of V_{maxcTF_i} (Figure 8A).

As opposed to gestation, the urinary clearance value was similar between the lactating and male rat. Thus, the value used in the postpartum human was the same value reported by Merrill et al. (2005a) for the nonpregnant adult. The model simulations of urinary iodide are consistent with the range of available data without parameter adjustment (Figure 8B). However, using the lower urinary clearance value from the gestation model does yield an improvement in the fit of the urine and thyroid (not shown).

Several studies have measured the amount of radioiodine in human milk. Together they provide a fairly complete time course for milk radioiodide concentration after an acute maternal dose (Dydek & Blue, 1988; Miller & Weetch, 1955; Nurnberger & Lipscomb, 1952; Rubow & Klopper, 1988; Weaver et al., 1960). The model accurately predicts the radioiodine content of human milk up to 5 d postdosing (Figure 8C).

Neonatal tissues. Available data in the neonate included thyroid radioiodide uptake and urinary iodide measurements. Predicted thyroid uptake after d 3 was tested against measured thyroid uptake in the newborn (<1 wk) (Figure 5) and neonate (PNM 1–12) after a single direct radioiodide dose to the child. Neither the measured nor the model predicted thyroid uptakes changed significantly after PND 4 (Figure 2). Model predicted thyroid iodide content varies from 25 to 26% of the total neonatal dose between wk 1 and mo 12, which is within the range of the data ($20 \pm 10\%$).

Neonatal urinary clearance is expected to increase with age as the kidneys mature. In this model, the kidney function was scaled from the adult parameter by $BW^{0.75}$. The predicted urinary output was tested against data in the newborn (PND 2 and 3) and in the older child (9 mo–12 yr) (Figure 9) following a single direct dose of radiolabeled iodide to the child. The data indicate the expected increase in urinary excretion with age, which is replicated by the model.

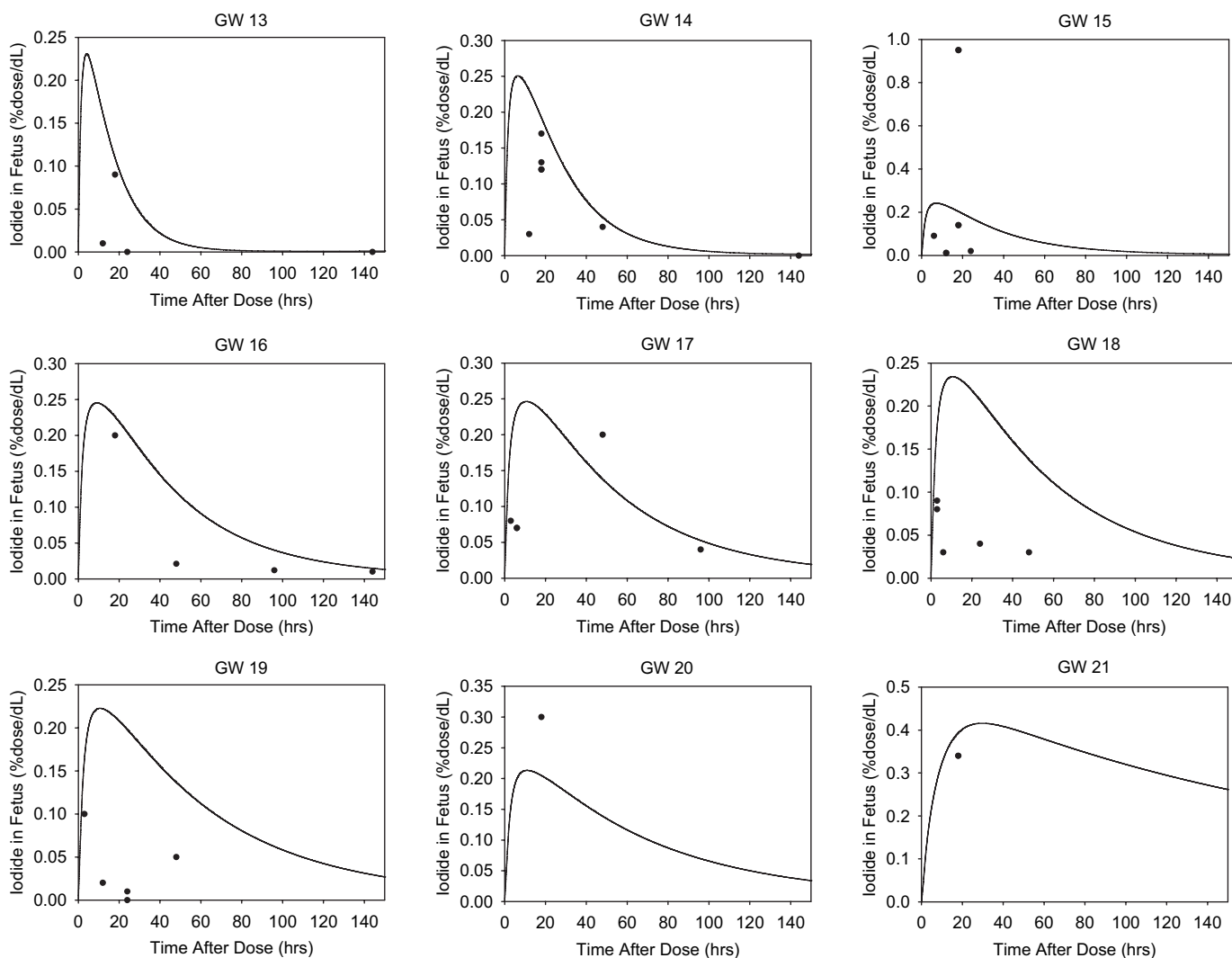


FIG. 7. Total fetal ¹³¹I⁻ burden. The model simulation is shown versus data from individual fetuses after iv dosing to the pregnant woman at 13, 14, 15, 16, 17, 18, 19, 22, and 23 wk of gestation (Aboul-Khair et al., 1966; Dyer & Brill, 1972).

Tissues from weaning to adolescence. The chemical-specific parameters in the child after weaning were set to those of the adult and adjusted for growth by allometric scaling ($BW^{0.75}$). After the first week, thyroid uptake and urinary clearance remain constant. Likewise, the model-predicted 24-h thyroid iodide uptake is consistently 25% of the total dose throughout childhood, with urinary iodide accounting for nearly all the remaining radioiodide.

Extrapolation to Perchlorate Exposure

Since few ClO₄⁻ data are available, extrapolation to human ClO₄⁻ kinetics was based on the assumption that if nearly identical models are able to describe both anions in the rat across life stages and in the adult human, and the same models are successfully extrapolated to the perinatal human for I⁻,

then the ClO₄⁻ model should also produce a reasonable estimate of the perinatal human. Epidemiological data were used to test this extrapolation. Two separate studies were performed in Chile where ClO₄⁻ is naturally occurring in the soil and, therefore, the drinking water. The first studied school children (Crump et al., 2000; Gibbs et al., 2004) and the second followed women through pregnancy and lactation (Tellez et al., 2005).

Tellez et al. (2005) collected serum and spot urine samples in pregnant women from three cities representing control (0 ppb), low (5.8 ± 0.6 ppb), and high (114 ± 13 ppb) ClO₄⁻ exposures, at their first (GW 15) and second (GW 33) prenatal visit. Serum ClO₄⁻ was only detectable in the high-exposure city. To simulate this exposure, the model was run at a continuous oral exposure throughout gestation. For each time point, the model was run at three doses representing the

TABLE 3
Model-Predicted $^{131}\text{I}^-$ in Fetal Tissues 18 h After Maternal Oral Administration at GW 14, 15, and 22 Versus the Measured Values of Dyer et al. (1969)

Week of gestation	Fetal tissue	Measured radioiodide (ng/L)	Predicted radioiodide (ng/L)	Predicted: observed Ratio
14	Thyroid	75	78	1.0
	Kidney	0.012	0.055	4.6
	GI	0.014	0.051	3.6
15	Thyroid	57/91	81	1.4/0.9
	Blood	0.053	0.048	0.9
	Kidney	0.031	0.052	1.7
	GI	0.032	0.048	1.5
22	Thyroid	249	157	0.6
	Blood	0.036	0.018	0.5
	Kidney	0.012	0.02	1.7
	GI	0.018	0.018	1.0

mean \pm one standard deviation (SD) of the reported maternal ClO_4^- exposure. Using the approach for parameter determination demonstrated with I^- , the model predicted an average serum concentration of $4 \pm 2 \mu\text{g/L}$ in the pregnant woman at both time points, which is roughly threefold less than the measured values.

In the nonpregnant adult model, Merrill and coauthors (2005a) fitted the ClO_4^- urinary clearance value to each individual for which ClO_4^- data were available and noted a marked variation between subjects. Values for urinary clearance (ClUC_p) ranged from 0.05 to 0.24 ng/L-h, with an average of 0.13 ng/L-h. Using the lower bound of these values (0.05 ng/L), the gestation model predicted serum levels were within the range of the experimental values of Tellez et al. (2005) (Figure 10). Since the lower clearance value lies within the range of the normal adult, improves the ClO_4^- prediction, and yields a more conservative estimate of risk, it was used for all subsequent maternal simulations and dose metric calculations.

Cord blood was also collected from the above subjects at the time of birth. The ClO_4^- concentration in cord blood of children from the high exposure city was nearly two times higher than had previously been measured in maternal blood (Tellez et al., 2005). The gestation model was able to predict the fetal ClO_4^- concentration at 38 wk (Figure 10).

Breast milk was collected from the same women at their postpartum checkup (5–6 wk). ClO_4^- was detected in milk from women residing in all three cities, including the controls, which the authors attributed to an unidentified second source. The model was run for the low- and high-dose populations. In both populations, model predictions lie within two SD of the data (Figure 11).

In 2000, a cohort of school children living in the same cities as those studied by Tellez et al. (2005) were examined for potential thyroid effects from ClO_4^- exposure (Crump et al., 2000). The serum and urine ClO_4^- levels in the children (average age = 7.4 yr) were reported by Gibbs et al. (2004). The neonatal model was given a constant ClO_4^- dose up to 7.4 yr to simulate the children's exposure. As described, chemical-specific parameters were scaled allometrically from the adult values of Merrill et al. (2005a). The model-predicted average serum concentration of $5.9 \mu\text{g/L}$ is nearly identical to the measured value ($5.6 \pm 1.8 \mu\text{g/L}$) without any parameter adjustment (Figure 10).

Calculation of Dose Metrics Across Life Stages

These models can provide quantitative estimates of two vital pieces of information for risk characterization: perinatal exposure and the relative sensitivity of exposed populations. In Figure 12, the model-predicted fetal and neonatal doses are compared to the corresponding maternal doses (per kg BW). The calculations were performed at several different time points between GW 12 (onset of fetal thyroid function) and the end of the first year of life. Fetal dose was consistently higher than maternal dose per kg BW, though the difference decreases over gestation (Figure 12A). The postnatal kinetics are more dynamic: at low maternal doses ($<0.1 \text{ mg/kg-d}$) the neonatal dose was generally higher (per kg BW) than the lactating woman's, while the opposite trend was seen at higher maternal doses (Figure 12B).

Dosimetrics were calculated at several hypothetical drinking water doses for two important determinants of risk: area under the curve (AUC) for ClO_4^- in the serum (Table 4) and

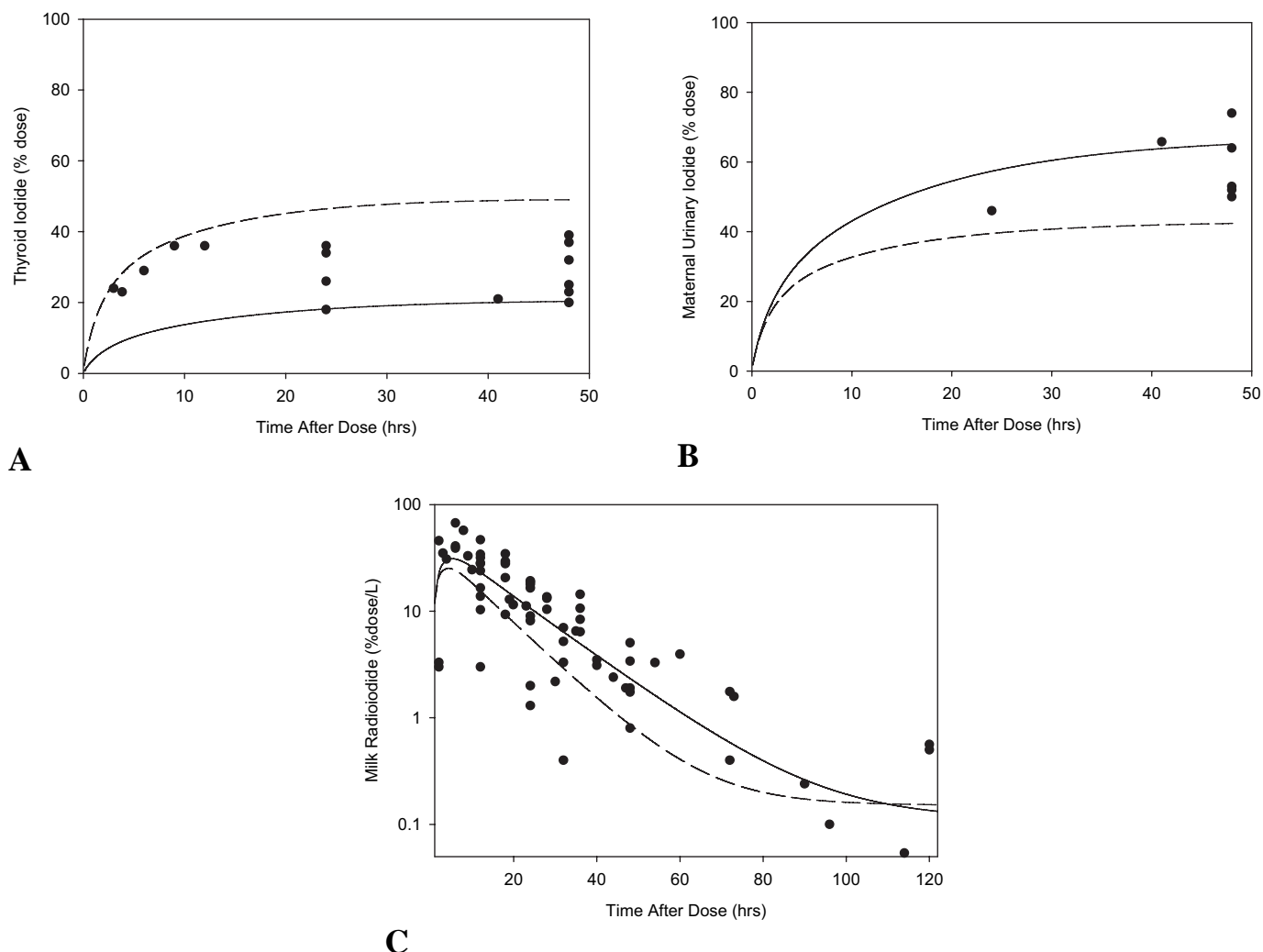


FIG. 8. Predicted radioiodide concentration in the (A) thyroid, (B) urine, and (C) breast milk of lactating women. Solid line and broken lines represent simulations performed using $V_{max}cT_i$ calculated from mean and maximal values reported for the nonpregnant adult in Merrill et al. (2005a). PBPK model was run at postpartum mo 4. Data points represent measurements in individual subjects for the thyroid (Dydek & Blue, 1988; Nurnberger & Lipscomb, 1952; Robinson et al., 1994; Weaver et al., 1960), urine (Weaver et al., 1960), and milk (Dydek & Blue, 1988; Miller & Weetch, 1955; Nurnberger & Lipscomb, 1952; Rubow & Klopper, 1988; Weaver et al., 1960), independent of postpartum month.

the percent inhibition of thyroid I⁻ uptake (Table 5). Maternal and fetal serum ClO₄⁻ AUCs did not change over gestation. In lactation, however, maternal AUCs peaked in the first postnatal week (PNM 0.25) and the neonate's AUC was highest in PNM 3. The values shown in Tables 4 and 5 represent the lactating woman and nursing infant in their most sensitive time points—PNM 0.25 and 3, respectively. At low external doses, the blood concentrations were highest in the fetus, followed closely by the lactating woman and neonate. In fact, at 0.001 mg/kg-d (approximately half that of the high exposure city in Chile), the serum of the fetus and the lactating woman and neonate are five- and fourfold higher than for the nonpregnant adult, respectively. At higher external doses, this trend ceases.

Thyroid inhibition predictions were obtained by administering a constant external ClO₄⁻ dose throughout gestation, lactation

and childhood, and simulating a single I⁻ dose 24 h prior to recording the total amount of iodine in the thyroid. Predicted fetal inhibition at the lowest dose was twofold greater than the nonpregnant adult (1 vs. 0.5%). Of the life stages, the nonpregnant adult and older child showed the least susceptibility to thyroid inhibition, while the fetus and lactating woman showed the most.

DISCUSSION

These models may help bridge the gap between observed effects in animals and potential risk to the human. Through the inclusion of known physiology and established descriptions of chemical transport, it is possible to logically and quantitatively estimate chemical behavior in biological systems that are not

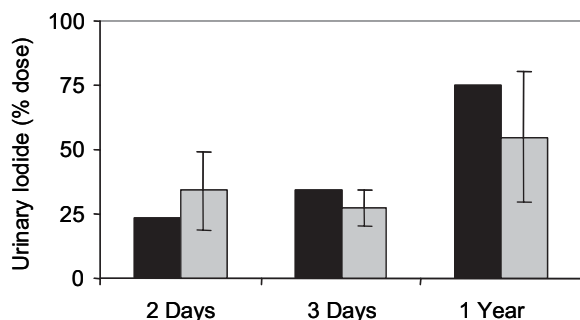


FIG. 9. Predicted radioiodide in neonatal urine after a direct oral $^{131}\text{I}^-$ dose. Black bars represent the model simulation. Gray bars represent the measured cumulative urine from individual subjects (Fisher & Oddie, 1964; Reilly & Bayer, 1952). SDs of measured data are indicated by the cross-bars. For the 1-yr simulation, data were taken from subjects varying from 9 mo to 12 yr of age.

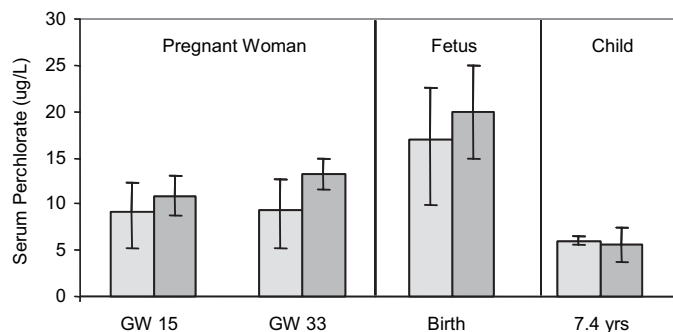


FIG. 10. Model predicted serum perchlorate in populations exposed to 114 ppm ClO_4^- in drinking water at different life stages. Predicted values (light gray) are shown for the average \pm SD of the reported dose. The mean measured values (dark gray) for serum ClO_4^- concentration \pm one SD were obtained from Tellez et al. (2005). The model predictions for gestation were obtained using the low end of the range of urinary clearance values reported in Merrill et al. (2005a).

easily measured. Several characteristics make ClO_4^- a suitable test chemical for such extrapolation. First, the anion is not metabolized *in vivo* and has very similar kinetics to inorganic I^- , which has been measured in various stages of human development. Second, a suite of models has previously been made available for various life stages in the rat and adult human that allows the estimation of life-stage- and species-specific differences in kinetic parameters (Clewell et al., 2003a, 2003b; Merrill et al., 2003, 2005a). Finally, the presence of ClO_4^- in drinking water, potential for thyroid disruption, and lack of perinatal human data highlight the need for an alternative, scientifically sound approach to determining human perinatal dosimetry.

The described model is able to predict iodide and perchlorate kinetics in the human from fetal life through adulthood. This allows the quantitative estimation of target tissue dose (i.e., developing thyroid). Using what information is available for the chemical mechanism (competitive inhibition of NIS), one can then use these models predictively to assess the risk of

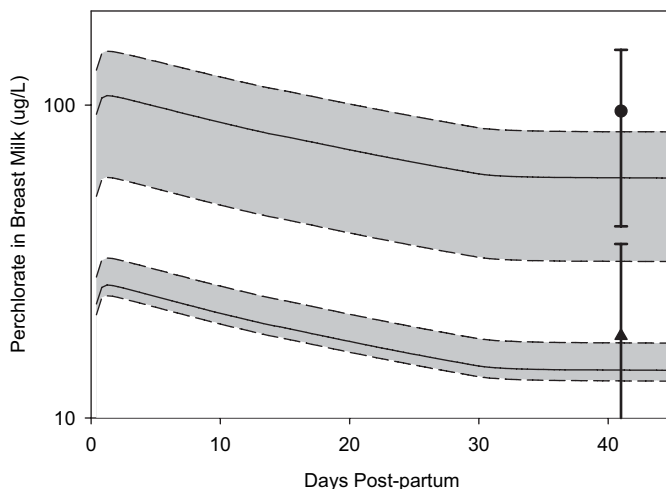


FIG. 11. Model-predicted perchlorate in breast milk from drinking-water exposure. Solid lines represent the model simulation at the mean estimated exposure. Broken lines represent the model simulations for exposures \pm one SD. Cross bars represent the mean \pm SD of measured perchlorate in breast milk from the cities with 5 (\blacktriangle) and 114 ppm (\bullet) perchlorate in the drinking water (Tellez et al., 2005).

biological effect (thyroid iodide inhibition) that precedes downstream toxicity.

The model successfully predicts iodide kinetics based on (1) validated structure of the perinatal rat models, (2) published physiological parameters, and (3) chemical-specific parameters estimated using the parallelogram approach. Other than thyroid activity in the fetus and newborn (≤ 3 d), it was not necessary to adjust estimated parameters to fit the data. This is not to suggest that model fit could not be improved; it is possible that better fits could be obtained through more focused parameter optimization. Analysis of probable distributions for the more sensitive parameters and their effect on model simulations would also be useful in risk assessment applications. Nonetheless, successful extrapolation of the model to predict human iodide data supports the use of this same paradigm with ClO_4^- .

Using the same approach predicts serum ClO_4^- concentrations within a factor of 3 from measured values. Yet, through careful examination of the more sensitive model parameters, it was noted that those governing urinary clearance of ClO_4^- had a rather significant range of suitable values in the nonpregnant human (Merrill et al., 2005a). Using the lower bound urinary clearance value to calculate the maternal parameter resulted in predicted serum ClO_4^- levels that agreed with measured values. A difference in excretion may account for observed differences in serum levels: <4 ppb in nonpregnant adults (Greer et al., 2002) versus 11–13 ppb in pregnant women (Tellez et al., 2005) at approximately the same ClO_4^- exposure.

The models showed reduced iodide clearance during gestation; it is possible that the same mechanism may prevent efficient ClO_4^- clearance. Serum ClO_4^- was elevated in the

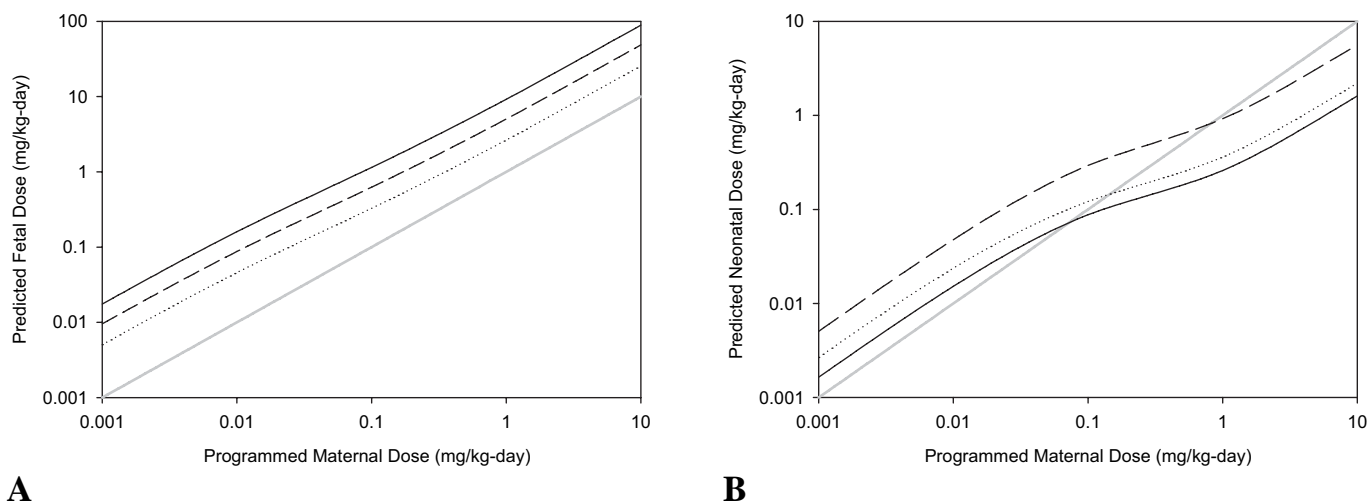


FIG. 12. Model predicted perchlorate dose to the (A) fetus and (B) neonate as a function of maternal dose. Model was run at early, mid, and late gestation and lactation with a constant maternal dose. The gray line is unity. The solid, broken, and dotted lines represent simulations at (A) wk 12, 18, and 38 in gestation and (B) mo 0.25, 3, and 9 in lactation, respectively.

TABLE 4
Model-Predicted Serum ClO₄⁻ Area Under the Curve (AUC) Across LifeStages

External dose (mg/kg-d)	Fetus ^a (mg/L)	Neonate ^b (mg/L)	Child (mg/L)	Adult (mg/L)	Pregnant ^a woman (mg/L)	Lactating ^c woman (mg/L)
0.001	0.010	0.008	0.001	0.002	0.005	0.008
0.01	0.06	0.05	0.01	0.01	0.04	0.05
0.1	0.2	0.2	0.1	0.1	0.3	0.3
1.0	1.2	0.5	0.8	1.0	2.5	2.5

^aFetus and pregnant woman shown at GW 38.

^bNeonate shown at PNM 1.5.

^cLactating woman shown at PND 7.

TABLE 5
Model Predicted Inhibition of Thyroid Iodide Uptake (% Inhibition) Across LifeStages

External dose (mg/kg-d)	Fetus ^a (% inhibition)	Neonate ^b (% inhibition)	Child (% inhibition)	Adult (% inhibition)	Pregnant ^a woman (% inhibition)	Lactating ^c woman (% inhibition)
0.001	1.1	0.9	0.3	0.6	1.0	1.1
0.01	10	8	3	4	9	10
0.1	49	34	21	31	50	54
1.0	84	63	72	81	91	92

^aFetus and pregnant woman shown at GW 38 (birth).

^bNeonate shown at PNM 1.5.

^cLactating woman shown at PND 7.

pregnant and lactating rat (Clewell et al., 2003a, 2003b). Since the data in the male rat suggested that protein binding dominated low-dose kinetics (Merrill et al., 2003), the elevated serum levels were attributed to plasma binding. The lack of acute ClO_4^- data in gestation and the marked influence of binding might have obscured the effect of changing clearance in the rat models. However, in the human where plasma binding of ClO_4^- is low, differences in urinary clearance would be more apparent.

The lower urinary clearance value was ultimately used in gestation and lactation. This was deemed appropriate because the value (1) is consistent with the previous human model, (2) agrees with the observed trend in iodine, and (3) provides a more conservative estimate of exposure. Without postpartum serum data, it is difficult to determine whether the decreased clearance is maintained in the lactating mother. However, it is likely that the compensatory mechanism would remain in place while considerable loss of iodine is occurring via the milk.

Using this adjusted value for urinary clearance, the model accurately describes maternal serum, cord blood and maternal milk ClO_4^- after ingestion of contaminated drinking water. In the study by Tellez and coauthors (2005), it was noted that a secondary exposure source existed. The authors used urinary clearance to reconstruct the total daily ClO_4^- dose and found a consistent additional (nondrinking water) dose of approximately 30 $\mu\text{g}/\text{d}$ in all of the cities in Chile. This second source was included in the model simulations. In the subjects where blood levels were available (high exposure city only), the second source accounted for only 20% of the ClO_4^- dose and had little effect on predicted serum and milk levels. In the low exposure city, however, the unidentified second source was approximately fivefold greater than the drinking-water exposure and predictions of the milk from this city depended on its inclusion. In older children, urinary ClO_4^- measurements were consistent with the exposure expected from drinking-water ingestion alone (Gibbs et al., 2004). The ability of the model to simulate differences in measured serum levels in the adult and older child with the same kinetic parameters suggests that the measured differences in ClO_4^- concentrations are probably due to variation in exposure and physiology. Thus, these models are expected to be useful in estimating ClO_4^- dosimetry across life stages.

Without the structure enforced by the mathematical descriptions of physiology and chemical kinetics, it would be necessary to rely on external dose as the estimate for fetal and neonatal exposure. Yet, with the exception of a few chemicals whose kinetics are truly governed by passive diffusion, external dose actually gives little indication of fetal or neonatal exposure. Using the model, the fetus was found to have consistently higher doses than the mother (per kg BW) due to several factors: placental NIS uptake, diffusion-limited placental transfer, the lack of plasma binding, and the low urinary clearance that makes more ClO_4^- available for placental transport. The apparent decline in fetal dose (per kg BW) over gestation is

likely due to the fairly constant placental transfer and the rapid fetal growth, that is, dilution.

At low external doses (<0.1 mg/kg-d), the neonatal dose is also greater than the mother's (per kg BW). However, at higher external doses, the opposite trend is seen. This is presumably due to the presence of NIS in the mammary gland. At lower doses, ClO_4^- is actively transferred to the neonate, but at higher doses the symporter is saturated. In this model and in the previous rat models (Clewell et al., 2003a, 2003b), uptake into the mammary gland appears to play a greater role in postnatal perchlorate and iodide kinetics than does the placenta in gestation. Mammary NIS is known to be upregulated by the hormones that promote lactation (Cho et al., 2000; Rillema et al., 2000). The role of NIS may be more important in lactation where little hormone is transferred to the neonate than in gestation where the mother provides much of the fetal thyroxine (Howdeshell, 2002; Mizuta et al., 1983).

Predicted serum ClO_4^- levels are higher in the perinatal time points than in the older child or nonpregnant adult, due to reduced maternal urinary clearance as described earlier. While serum ClO_4^- is always higher in the pregnant and lactating woman than in the nonpregnant adult, the concentrations peak in the first postpartum week, while milk production is still low. When milk production increases, greater clearance causes maternal serum levels to fall.

Fetal serum ClO_4^- levels showed the highest ClO_4^- concentrations, which is consistent with the data. This represents a significant species difference in ClO_4^- kinetics. In the rat, the fetal serum ClO_4^- levels were approximately half those of the dam (Clewell et al., 2003b), and the lactating female had the highest serum ClO_4^- concentration. This different dosimetry results from the species differences in binding. The high binding in the rat traps ClO_4^- in the maternal serum, and limits NIS transport, suggesting a protective role for plasma binding in rat development. In the human, the lack of serum binding coupled with the reduced maternal urinary clearance, increases the amount of free ClO_4^- that is available for NIS transport. Serum levels of ClO_4^- are therefore higher in the human fetus than would have been predicted from rat models.

The differential response in the hypothalamus–pituitary–thyroid (H-P-T) axis in the rat and human after ClO_4^- exposure prohibits a direct comparison of hormone effects. However, the similarity in NIS inhibition across species allows the comparison of this precursor effect. The models were used to predict inhibition of thyroid I^- uptake across life stages through competition for NIS binding sites. Ideally, the model would be validated against all important endpoints (ClO_4^- concentration, I^- inhibition in the fetal/neonatal thyroid, etc.). However, since inhibition was not measured in the perinatal human, these predictions cannot be tested directly. The ability of models with the same structure and nearly identical parameters to predict inhibition in the adult human and across life stages in the rat indicates that this is a reasonable application of the model.

No description of upregulation was included in the model, based on the fact that upregulation was not seen in the non-pregnant adult after 2 wk of doses as high as 1 mg ClO₄⁻ (Merrill et al., 2005a). Though the current simulations cover lifetime exposures rather than a few weeks, the accompanying data on thyroid hormones (TSH, T₄) still do not show evidence of thyroidal upregulation (Crump et al., 2000; Tellez et al., 2005). Like the previous serum ClO₄⁻ AUC calculations, the model estimates of thyroid iodide inhibition suggest that fetal development may be the most sensitive life stage.

It is interesting that predicted thyroid iodide inhibition is greater in the fetus than in the neonate, since ClO₄⁻ interferes with mammary NIS, and the mammary gland appears to play such a dominant role in iodide kinetics during lactation. Analysis of the model behavior may help explain this behavior. Normally, thyroid uptake dominates iodide kinetics due to the high NIS capacity and ability to trap iodide in the colloid. The fast, efficient removal from the blood drives peripheral tissue kinetics. When thyroid iodide uptake is inhibited, the serum levels increase significantly, making more I⁻ available to the mammary gland (or placenta) (see Figures 6 and 8). The mammary gland has a second I⁻ (Pendrin) transporter (Rillema & Hill, 2003) and is able to incorporate iodide into hormone precursors, effectively trapping the iodine in the milk. Thus, it is not surprising that when maternal thyroid uptake is diminished, these specialized processes help protect the neonate against inhibition. Indeed, in the first week of lactation when milk production is low, the model predicts an increase in thyroid iodide uptake at low ClO₄⁻ doses. At higher doses, enough ClO₄⁻ is present to negate this effect.

Predicted inhibition in all perinatal time points were notably higher than in either the nonpregnant adult or older child. This is a direct result of the increased serum ClO₄⁻ levels, though the nonlinear NIS activity and different thyroidal clearance of the two anions results in just a threefold difference in inhibition with a fivefold increase in serum ClO₄⁻ (0.001 mg/kg-d). The final predicted fetal inhibition is approximately 1% at environmentally relevant doses. In the studies of Greer et al. (2002), measured inhibition was not statistically significant in euthyroid individuals with sufficient iodine intake until it was greater than approximately 10%, due to the degree of interindividual variability in thyroid uptake. In order to reach this level of inhibition in the fetus, the model predicts a necessary maternal dose of 0.01 mg/kg-d. This is approximately 5 times greater than the exposure of the Chilean women (Tellez et al., 2005) and nearly 15 times greater than reference dose adopted by the U.S. Environmental Protection Agency (U.S. EPA, 2005).

One of the inherent flaws in extrapolating human perinatal risk from animal data is the difference in timing of development: Many processes that occur in the rat after birth take place in utero in the human. PBPK models are used to determine the target tissue dose (i.e., serum concentration) associated with an observed effect in the rat at a specific time point and translate it into an administered dose (exposure) at the corresponding

developmental period in the human. In this way, one can begin to tease out the impact of pharmacokinetic and pharmacodynamic differences between species. Here, species differences in serum ClO₄⁻ binding and urinary clearance of both anions led to considerably different predictions of fetal dose and susceptibility from a kinetic standpoint. However, one has yet to begin the task of quantifying the pharmacodynamic differences between rat and human response to ClO₄⁻ exposure.

Several important differences are known to exist between the rat and human endocrine system. Perhaps most important is the large capacity for iodine storage in the human through hormone binding to TBG in serum and increased colloid capacity (Merrill et al., 2005a). The timing of the H-P-T axis development is also significantly different between species. The rat thyroid begins producing hormones just 3 d before birth; the human thyroid is active by wk 13 of gestation (Bernal et al., 1984; Porterfield, 1994; Roti et al., 1983). Furthermore, much of the thyroid-dependent brain development occurs in utero in the human, while the same processes take place in the postnatal rat (Howdeshell, 2002). This may have a significant effect on children's risk, due to the difference between thyroid hormone kinetics in gestation and lactation. During gestation, maternal thyroid hormones contribute significantly to fetal levels even after the onset of fetal thyroid function (Contempré et al., 1993; Vulmsa et al., 1989). However, after parturition, the neonate must synthesize its own hormones from inorganic I⁻ supplied in the milk (Etling & Gehin-Fouque, 1984; Mizuta et al., 1983; van Wassenaeer et al., 2002). Thus, the maternal hormone supply may protect the human fetus in the presence of thyroid inhibitors, and the neonate could be the more vulnerable population. Factors such as congenital hypothyroidism and maternal hypothyroidism, which are fairly common in the United States (Allan et al., 2000), further confound this issue.

The delicacy of the developing endocrine system and its dependence on environmental, congenital, and maternal factors suggest that translating the rat effect data to exposure levels in human children requires a better understanding of the pharmacodynamics of thyroid hormone homeostasis and perturbation through thyroid inhibition. A few efforts have been made recently to expand the published perchlorate and iodide models to account for hormone changes in the adult human (Fisher et al., 2005) and rat (Merrill et al., 2005b). Through thorough testing, validation, and elaboration of these models to describe perinatal dynamics, one can continue to improve predictions of perinatal risk.

REFERENCES

- Aboul-Khair, S. A., Buchanan, T. J., Crooks, J., and Turnbull, A. C. 1966. Structural and functional development of the foetal thyroid. *Clin. Sci.* 31:415-424.
- Allan, W. C., Haddow, J. E., Palomaki, G. E., Williams, J. R., Mitchell, M. L., Hermos, R. J., Faix, J. D., Klein, R. Z. 2000. Maternal thyroid deficiency and pregnancy complications: Implications for population screening. *J. Med. Screen.* 7:127-130.

- Bernal, J., Perez-Castillo, A., Pans, T., and Pekonen, F. 1984. Ontogenesis of thyroid hormone receptor. In *Endocrinology: Proceedings of the 7th International Congress of Endocrinology, Quebec City, 1-7 July 1984*, eds. F. Labrie and L. Proulx, pp. 977-980. Excerpta Medica, New York.
- Bocian-Sobkowska, J., Malendowicz, L. K., and Wozniak, W. 1992. Morphometric studies on the development of human thyroid gland in early fetal life. *Histol. Histopathol.* 7:415-420.
- Bocian-Sobkowska, J., Wozniak, W., and Malendowicz, L. K. 1997. Morphometric studies on the development of the human thyroid gland. II. The late fetal life. *Histol. Histopathol.* 12:79-84.
- Brabant, G., Bergmann, P., Kirsch, C. M., Kohrle, J., Hesch, R. D., and von zur Muhlen, A. 1992. Early adaptation of thyrotropin and thyroglobulin secretion to experimentally decreased iodine supply in man. *Metab. Clin. Exp.* 41:1093-1096.
- Braverman, L. E., Pearce, E. N., He, X., Pino, S. et al. 2006. Effects of six months of daily low-dose perchlorate exposure on thyroid function in healthy volunteers. *J. Clin. Endocrinol. Metab.* 91(7):2721-2724.
- Brines, J. K., Gibson, J. G., and Kunkel, P. 1941. The blood volume in normal infants and children. *J. Pediatr.* 18:447-457.
- Brown, R. A., Al-Moussa, M., Swanson Beck, J. 1986. Histometry of normal thyroid in man. *J. Clin. Pathol.* 39:475-482.
- Brown-Grant, K. 1961. Extrathyroidal iodide concentrating mechanisms. *Physiol. Rev.* 41:189-213.
- Brown-Grant, K., and Pethes, G. 1959. Concentration of radioiodine in the skin of the rat. *J. Physiol.* 148:683-693.
- Caron, P., Hoff, M., Bazzi, S., Dufor, A., Faure, G., Ghandour, I., Lauzu, P., Lucas, Y., Maraval, D., Mignot, F., Ressigeac, P., Vertongen, F., and Grange, V. 1997. Urinary iodine excretion during normal pregnancy in healthy women living in the southwest of France: Correlation with maternal thyroid parameters. *Thyroid* 7:749-754.
- Chapman, E. M., Corner, G. W., Robinson, D., and Evans, R. D. 1948. The collection of radioactive iodine by the human fetal thyroid. *J. Clin. Endocrinol.* 8:717-720.
- Cho, J. Y., Leveille, R., Kao, R., Rousset, B., Parlow, A. F., Burak, W. E. Jr., Mazzaferri, E. L., and Jhiang, S. M. 2000. Hormonal regulation of radioiodide uptake activity and Na⁺-I⁻ symporter expression in mammary glands. *Endocrinology* 85:2936-2943.
- Clewell, H. J., Gentry, P. R., Covington, T. R., Sarangapani, R., and Teeguarden, J. G. 2004. Evaluation of the potential impact of age- and gender-specific pharmacokinetic differences on tissue dosimetry. *Toxicol. Sci.* 79:381-393.
- Clewell, R. A., Merrill, E. A., and Robinson, P. J. 2001. The use of physiologically based models to integrate diverse data sets and reduce uncertainty in the prediction of perchlorate and iodide kinetics across life stages and species. *Toxicol. Ind. Health* 17:210-222.
- Clewell, R. A., Merrill, E. A., Yu, K. O., Mahle, D. A., Sterner, T. R., Fisher, J. W., and Gearhart, J. M. 2003a. Predicting neonatal perchlorate dose and inhibition of iodide kinetics in the rat during lactation using physiologically based pharmacokinetic modeling. *Toxicol. Sci.* 74:416-436.
- Clewell, R. A., Merrill, E. A., Yu, K. O., Mahle, D. A., Sterner, T. R., Mattie, D. R., Robinson, P. J., Fisher, J. W., and Gearhart, J. M. 2003b. Predicting fetal perchlorate dose and inhibition of iodide kinetics in gestation: A physiologically based pharmacokinetic analysis of perchlorate and iodide kinetics in the rat. *Toxicol. Sci.* 73:235-255.
- Collette, T. W., Williams, T. L., Urbansky, E. T., Magnuson, M. L., Hebert, G. N., Strauss, S. H. 2003. Analysis of hydroponic fertilizer matrixes for perchlorate: Comparison of analytical techniques. *Analyst* 128:88-97.
- Contempré, B., Jauniaux, E., Calvo, R., Jurkovic, D., Campbell, S., de Escobar, G. M. 1993. Detection of thyroid hormones in human embryonic cavities during the first trimester of pregnancy. *J. Clin. Endocrinol. Metab.* 77:1719-1722.
- Crump, C., Michaud, P., Tellez, R., Reyes, C., Gonzalez, G., Montgomery, E. L., Crump, K. S., Lobo, G., Becerra, C., and Gibbs, J. P. 2000. Does perchlorate in drinking water affect thyroid function in newborns or school-age children? *J. Occup. Environ. Med.* 42:603-612.
- Dasgupta, P. K., Martinelango, P. K., Jackson, W. A., Anderson, T. A., Tian, K., Tock, R. W., and Rajagopalan, S. 2005. The origin of naturally occurring perchlorate: the role of atmospheric processes. *Environ. Sci. Technol.* 39:1569-1575.
- Delange, F. 2000. The role of iodine in brain development. *Proc. Nutr. Soc.* 59, 75-79.
- Dyde, G. J., and Blue, P. W. 1988. Human breast milk excretion of iodine-131 following diagnostic and therapeutic administration to a lactating patient with Graves' disease. *J. Nucl. Med.* 29:407-410.
- Dyer, N. C., and Brill, A. B. 1972. Maternal fetal transport of iron and iodide in human subjects. *Adv. Exp. Med. Biol.* 27:351-366.
- Dyer, N. C., Brill, A. B., Glasser, S. R., and Goss, D. A. 1969. Maternal-fetal transport and distribution of ⁵⁹Fe and ¹³¹I in humans. *Am. J. Obstet. Gynecol.* 103:290-296.
- Etlings, N., and Gehin-Fouque, F. 1984. Iodinated compounds and thyroxine binding to albumin in human breast milk. *Pediatr. Res.* 18:901-903.
- Evans, T. C., Kretzschmar, R. M., Hodges, R. E., and Song, C. W. 1967. Radioiodine uptake studies of the human fetal thyroid. *J. Nucl. Med.* 8:157-165.
- Fisher, D. A., and Nelson, J. C. 2001. Endocrine testing and treatment. In *Endocrinology*, eds. L. J. Degroot, J. L. Jameson, and W. D. Odell, Eds., 4th ed., p. 2592. Philadelphia: W. B. Saunders.
- Fisher, D. A., and Oddie, T. H. 1964. Comparison of thyroidal iodine accumulation and thyroxine secretion in euthyroid subjects. *J. Clin. Endocrinol. Metab.* 24:1143-1154.
- Fisher, D. A., Oddie, T. H., and Burroughs, J. C. 1962. Thyroidal radioiodine uptake rate measurement in infants. *Am. J. Dis. Child.* 103:738-749.
- Fisher, J. W., Campbell, J. L., and Guth, D. 2005. A human dietary iodide PBPK model to evaluate the effects of perchlorate on thyroidal iodide content. *Toxicol. Sci.* 84(suppl. 1):869 (abstr.).
- Gentry P. R., Covington, T. R., Andersen, M. E., and Clewell, H. J. 2002. Application of a physiologically-based pharmacokinetic model for isopropanol in the derivation of an RfD/RfC. *Regul. Toxicol. Pharmacol.* 36:51-68.
- Gibbs, J. P., Ahmad, R., Crump, K. S., Houck, D. P., Leveille, T. S., Findley, J. E., and Francis, M. 1998. Evaluation of a population with occupational exposure to airborne ammonium perchlorate for possible acute or chronic effects on thyroid function. *J. Occup. Environ. Med.* 40:1072-1082.
- Gibbs, J. P., Narayanan, L., and Mattie, D. R. 2004. Crump et al. study among school children in Chile: Subsequent urine and serum perchlorate levels are consistent with perchlorate in water in Taltal. *J. Occup. Environ. Med.* 46:516-517.
- Ginsberg, G., and Rice, D. 2005. The NAS perchlorate review: Questions remain about the perchlorate RfD. *Environ. Health Perspect.*, 113(11): 1117-1119.
- Gluzman, B. E., and Niepomniszcze, H. 1983. Kinetics of the iodide trapping mechanism in normal and pathological human thyroid slices. *Acta Endocrinol.* 103:34-39.
- Greer, M. A., Goodman, G., Pleus, R. C., and Greer, S. E. 2002. Health effects assessment for environmental perchlorate contamination: the dose response for inhibition of thyroidal radioiodine uptake in humans. *Environ. Health Perspect.* 110:927-937.
- Haddad, S., Restieri, C., and Krishnan, K. 2001. Characterization of age-related changes in body weight and organ weights from birth to adolescence in humans. *J. Toxicol. Environ. Health A.*, 64:453-464.
- Haddow, J. E., Palomaki, G. E., Allan, W. C., Williams, J. R., Knight, G. J., Gagnon, J., O'Heir, C. E., Mitchell, M. L., Hermos, R. J., Waisbren, S. E., Faix, J. D., and Klein, R. Z. 1999. Maternal thyroid deficiency during pregnancy and subsequent neuropsychological development of the child. *N. Engl. J. Med.* 341:549-555.
- Halmi, N. S., and Stuelke, R. G. 1959. Comparison of thyroidal and gastric iodide pumps in rats. *Endocrinology* 64:103-109.
- Hetzl, B. S., and Dunn, J. T. 1989. The iodine deficiency disorders: Their nature and prevention. *Annu. Rev. Nutr.* 9:21-38.
- Hodges, R. E., Evans, T. C., Bradbury, J. T., and Keettel, W. C. 1955. The accumulation of radioactive iodine by human fetal thyroids. *J. Clin. Endocrinol. Metab.* 15:661-667.
- Howdeshell, K. L. 2002. A model of the brain as a construct of the thyroid system. *Environ. Health Perspect.* 110(S3):337-348.

- Jackson, W. A., Joseph, P., Laxman, P., Tan, K., Smith, P. N., Yu, L., and Anderson, T. A. 2005. Perchlorate accumulation in forage and edible vegetation. *J. Agric. Food Chem.* 53:369–373.
- Kearns, J. F., and Philipsborn, H. F. 1962. Values for the thyroid uptake of I¹³¹ and protein-bound iodine in “normal” individuals from birth to twenty years. *Q. Bull. Northwest. Univ. Med. Sch.* 36:47–50.
- Kirk, A. B., Martinelango, P. K., Tian, K., Dutta, A., Smith, E. E., and Dasgupta, P. K. 2005. Perchlorate and iodide in dairy and breast milk. *Environ. Sci. Technol.* 39:2011–2017.
- Klein, A. H., Meltzer, S., and Kenny, F. M., 1972. Improved prognosis in congenital hypothyroidism treated before age three months. *J. Pediatr.* 81:912–915.
- Kotani, T., Ogata, Y., Yamamoto, I., Aratake, Y., Kawano, J. I., Suganuma, T., and Ohtaki, S. 1998. Characterization of gastric Na⁺/I⁻ symporter of the rat. *Clin. Immunol. Immunopathol.* 89:271–278.
- Kurz, H., Mauser-Ganshorn, A., and Stickel, H. H. 1977. Differences in the binding of drugs to plasma proteins from newborn and adult man. I. *Eur. J. Clin. Pharmacol.* 11:463–467.
- Martmer, E. E., Corrigan, K. E., Charbeneau, H. P., and Sosin, A. 1956. A study of the uptake of iodine (I-131) by the thyroid of premature infants. *Pediatrics* 17:503–508.
- Merrill, E. A., Clewell, R. A., Gearhart, J. M., Robinson, P. J., Sterner, T. R., Yu, K. O., and Fisher, J. W. 2003. PBPK predictions of perchlorate distribution and its effect on thyroid uptake of radioiodide in the male rat. *Toxicol. Sci.* 73:256–269.
- Merrill, E. A., Clewell, R. A., Robinson, P. J., Jarabek, A. M., Gearhart, J. M., Sterner, T. R., and Fisher, J. W. 2005a. PBPK model for radioactive iodide and perchlorate kinetics and the perchlorate-induced inhibition of iodide uptake in humans. *Toxicol. Sci.* 83:25–43.
- Merrill, E. A., Gearhart, J. M., Robinson, P. J., Sterner, T. R., and Mattie, D. R. 2005b. Preliminary development of a mechanistic thyroid hormone model. *Toxicol. Sci.* 84(suppl. 1):1305 (abstr.).
- Miller, H., and Weetch, R. S. 1955. The excretion of radioactive iodine in human milk. *Lancet* 269:1013.
- Mitchell, A. M., Manley, S. W., Morris, J. C., Powell, K. A., Bergert, E. R., and Mortimer, R. H. 2001. Sodium iodide symporter (NIS) gene expression in human placenta. *Placenta* 22:256–258.
- Mizuta, H., Amino, N., Ichihara, K., Harada, T., Nose, O., Tanizawa, O., and Miyai, K. (1983). Thyroid hormones in human milk and their influence on thyroid function of breast-fed babies. *Pediatr. Res.* 17:468–471.
- Motzer, W. E. 2001. Perchlorate: Problems, detection, and solutions. *Environ. Forens.* 2:301–311.
- National Research Council. 2005. *Health implications of perchlorate ingestion*. Washington, DC: National Academy Press.
- Nurnberger, C. E., and Lipscomb, A. L. 1952. Transmission of radioiodine (I¹³¹) to infants through human maternal milk. *J. Am. Med. Assoc.* 150:1398–1400.
- Ogborn, R. E., Waggenger, R. E., and VanHove, E. 1960. Radioactive-iodine concentration in thyroid glands of newborn infants. *Pediatrics* 26: 771–776.
- Ogiu, N., Nakamura, Y., Ijiri, I., Hiraiwa, K., and Ogiu, T. 1997. A statistical analysis of the internal organ weights of normal Japanese people. *Health Phys.* 72:368–383.
- Oliner, L., Kohlenbrener, R. M., Fields, T., and Kunstadter, R. H. 1957. Thyroid function studies in children: normal values for thyroidal I¹³¹ uptake and PBI¹³¹ levels up to the age of 18. *J. Clin. Endocrinol.* 17:61–75.
- Porterfield, S. P. 1994. Vulnerability of the developing brain to thyroid abnormalities: environmental insults to the thyroid system. *Environ. Health Perspect.* 102(suppl. 2):125–130.
- Quimby, E. H., and McCune, D. J. 1947. Uptake of radioactive iodine by the normal and disordered thyroid gland in children. *Radiology* 49:201–205.
- Reilly, W. A., and Bayer, D. I. 1952. The value of the measurements of thyroid uptake and urinary excretion of I¹³¹ in assessing thyroid function of normal and congenitally hypothyroid children. *J. Pediatr.* 40:714–721.
- Rillema, J. A., and Hill, M. A. 2003. Prolactin regulation of the pendrin-iodide transporter in the mammary gland. *Am. J. Physiol. Endocrinol. Metab.* 284:E25–E28.
- Rillema, J. A., Yu, T. X., and Jhiang, S. M. 2000. Effect of prolactin on sodium iodide symporter expression in mouse mammary gland explants. *Am. J. Physiol. Endocrinol. Metab.* 279:E769–E772.
- Robinson, P. S., Barker, P., Campbell, A., Henson, P., Surveyor, I., and Young, P. R. 1994. Iodine-131 in breast milk following therapy for thyroid carcinoma. *J. Nucl. Med.* 35:1797–1801.
- Roti, E., Gnudi, A., and Braverman, L. E. 1983. The placental transport, synthesis and metabolism of hormones and drugs which affect thyroid function. *Endocrine Rev.* 4:131–149.
- Rubow, S., and Klopper, J. 1988. Excretion of radioiodine in human milk following a therapeutic dose of I-131. *Eur. J. Nucl. Med.* 14:632–633.
- Shipp, A., Gentry, P. R., Lawrence, G. L., Van Landingham, C., Covington, T., Clewell, H. J., Gribben, K., and Crump, K. 2000. Determination of site-specific reference dose for methylmercury for fish-eating populations. *Toxicol. Ind. Health* 16(appendix B):420.
- Spitzweg, C., Joba, W., Eisenmenger, W., and Heufelder, A. E. 1998. Analysis of human sodium iodide symporter gene expression in extrathyroidal tissues and cloning of its complementary deoxyribonucleic acids from salivary gland, mammary gland, and gastric mucosa. *J. Clin. Endocrinol. Metab.* 83:1746–1751.
- Sternberg, J. 1973. Radiation risk in pregnancy. *Clin. Obstet. Gynecol.* 16, 235–278.
- Stewart, C. F., and Hampton, E. M. 1987. Effect of maturation on drug disposition in pediatric patients. *Clin. Pharmacol.* 6:548–564.
- Tazebay, U. H., Wapnir, I. L., Levy, O., Dohan, O., Zuckier, L. S., Zhao, Q. H., Deng, H. F., Amenta, P. S., Fineberg, S., Pestell, R. G., and Carrasco, N. 2000. The mammary gland iodide transporter is expressed during lactation and in breast cancer. *Nat. Med.* 6:871–878.
- Tellez, R. T., Chacon, P. M., Abarca, C. R., Blount, B. C., Van Landingham, C. B., Crump, K. S., and Gibbs, J. P. 2005. Chronic environmental exposure to perchlorate through drinking water and thyroid function during pregnancy and in the neonatal period. *Thyroid* 15(9):963–975.
- Thuett, K. A., Roots, E. H., Mitchell, L. P., Gentles, B. A., Andersen, T., Kendall, R. J., and Smith, E. E. 2002a. Effects of in utero and lactational ammonium perchlorate exposure on thyroid gland histology and thyroid and sex hormones in developing deer mice (*Peromyscus maniculatus*) through postnatal day 21. *J. Toxicol. Environ. Health A* 65:2119–2130.
- Thuett, K. A., Roots, E. H., Mitchell, L. P., Gentles, B. A., Andersen, T., and Smith, E. E. 2002b. In utero and lactational exposure to ammonium perchlorate in drinking water: Effects on developing deer mice at postnatal day 21. *J. Toxicol. Environ. Health A* 65:1061–1076.
- U.S. Environmental Protection Agency. 2003. Disposition of comments and recommendations for revisions to “Perchlorate environmental contamination: Toxicology review and risk characterization (External Review Draft, January 16, 2003).” Washington, DC: Office of Research and Development. EPA/600/R-03/031.
- U.S. Environmental Protection Agency. 2005. Integrated Risk Information System (IRIS) summary for perchlorate and perchlorate salts. National Center for Exposure and Assessment, Cincinnati, OH. <http://www.epa.gov/iris/subst/1007.htm>. Accessed 22 June 2005.
- U.S. Food and Drug Administration. 2004. Exploratory data on perchlorate in food. Available at <http://www.cfsan.fda.gov/~dms/clo4data.html>. Accessed 22 June 2005.
- Van Dilla, M. A., and Fulwyler, M. J. 1964. Radioiodine metabolism in children and adults after the ingestion of very small doses. *Science* 144:178–179.
- van Middlesworth, L. 1954. Radioactive iodide uptake of normal newborn infants. *Am. J. Dis. Child.* 88:439–442.
- van Middlesworth, L., Tuttle, A. H., and Threlkeld, A. 1953. Iodinated protein in milk. *Science* 118:749.
- van Wassenaer, A. G., Stulp, M. R., Valianpour, F., Tamminga, P., Ris Stalpers, C., de Randamie, J. S., van Beusekom, C., and de Vijlder, J. J. 2002. The quantity of thyroid hormone in human milk is too low to influence plasma thyroid hormone levels in the very preterm infant. *Clin. Endocrinol. (Oxf.)* 56:621–627.
- Vulsma, T., Gons, M. H., and de Vijlder, J. J. 1989. Maternal-fetal transfer of thyroxine in congenital hypothyroidism due to a total organification defect or thyroid agenesis. *N. Engl. J. Med.* 321:13–16.

- Weaver, J. C., Kamm, M. L., and Dobson, R. L. 1960. Excretion of radioiodine in human milk. *J. Am. Med. Assoc.* 173:872–875.
- Wellman, H. N., Kereiakes, J. G., and Branson, B. M. 1970. Total- and partial-body counting of children for radiopharmaceutical dosimetry data. In *Medical radionuclides: Radiation dose and effects*, eds. R. J. Clouter, C. L. Edwards, and W. S. Snyder, pp. 133–156. U.S. Public Health Service and U.S. Atomic Energy Commission. Washington, D.C.
- Wolff, J. 1998. Perchlorate and the thyroid gland. *Pharmacol. Rev.* 50:89–105.
- Yu, K. O., Narayanan, L., Mattie, D. R., Godfrey, R. J., Todd, P. N., Sterner, T. R., Mahle, D. A., Lumpkin, M. H., and Fisher, J. W. 2002. The pharmacokinetics of perchlorate and its effect on the hypothalamus-pituitary-thyroid axis in the male rat. *Toxicol. Appl. Pharmacol.* 182:148–159.

APPENDIX: MODEL EQUATIONS

Only equations developed from the literature data specifically for the human perinatal models are given here. See text for references to other equations.

Thyroid growth. Bocian-Sobkowska and coauthors (1992, 1997) measured thyroid weights and fractional volumes of the sub-compartments in fetuses aged 10 to 20 wk and 22 to 40 wk. To determine the relationship of the fetal thyroid growth to the total fetal growth, the relative thyroid volumes (as % BW) were plotted against fetal age. A polynomial equation was fit to the data in Microsoft Excel [Eq. (A1)] and then used in the model to simulate the growth of the fetal thyroid over time

after GW 10. Prior to GW 10, the volume was not measured and was therefore scaled by BW from the earliest measured time point (GW 10). Relative volume of the stroma and follicle (VTBc and VTFc) were also reported for the fetal thyroid in these papers. These fractions were programmed into the model using a TABLE function, which employs linear interpolation between data points. The volume of the thyroid lumen (VTL) was determined by subtracting the volume of the stroma and follicle from the total thyroid volume. Ogiu et al. (1997) measured total thyroid volume in children aged 1 to 17 yr. The equation describing the change in fractional thyroid volume (/kg BW) is given in Eq. (A2). Fractional volumes of the stroma, follicle and colloid (per kg thyroid) were obtained for birth (Bocian-Sobkowska et al., 1992) and 1 to 17 yr (Brown et al., 1986).

$$V_{tot_F} = -3 \times 10^{-14} (\text{hours}^3) + 5 \times 10^{-10} (\text{hours}^2) - 2 \times 10^{-6} (\text{hours}) + 0.0033 \quad [A1]$$

$$V_{tot_N} = 0.63 \times \text{months} + 1.3857 \quad [A2]$$

where V_{tot_F} and V_{tot_N} are the fractional volumes for the total thyroid (L/kg BW) in the fetus and neonate, respectively.